

Sun-as-a-star observations to characterize stellar active regions and universal atmospheric heating mechanism

Shin Toriumi

Japan Aerospace Exploration Agency (JAXA)

1. Introduction

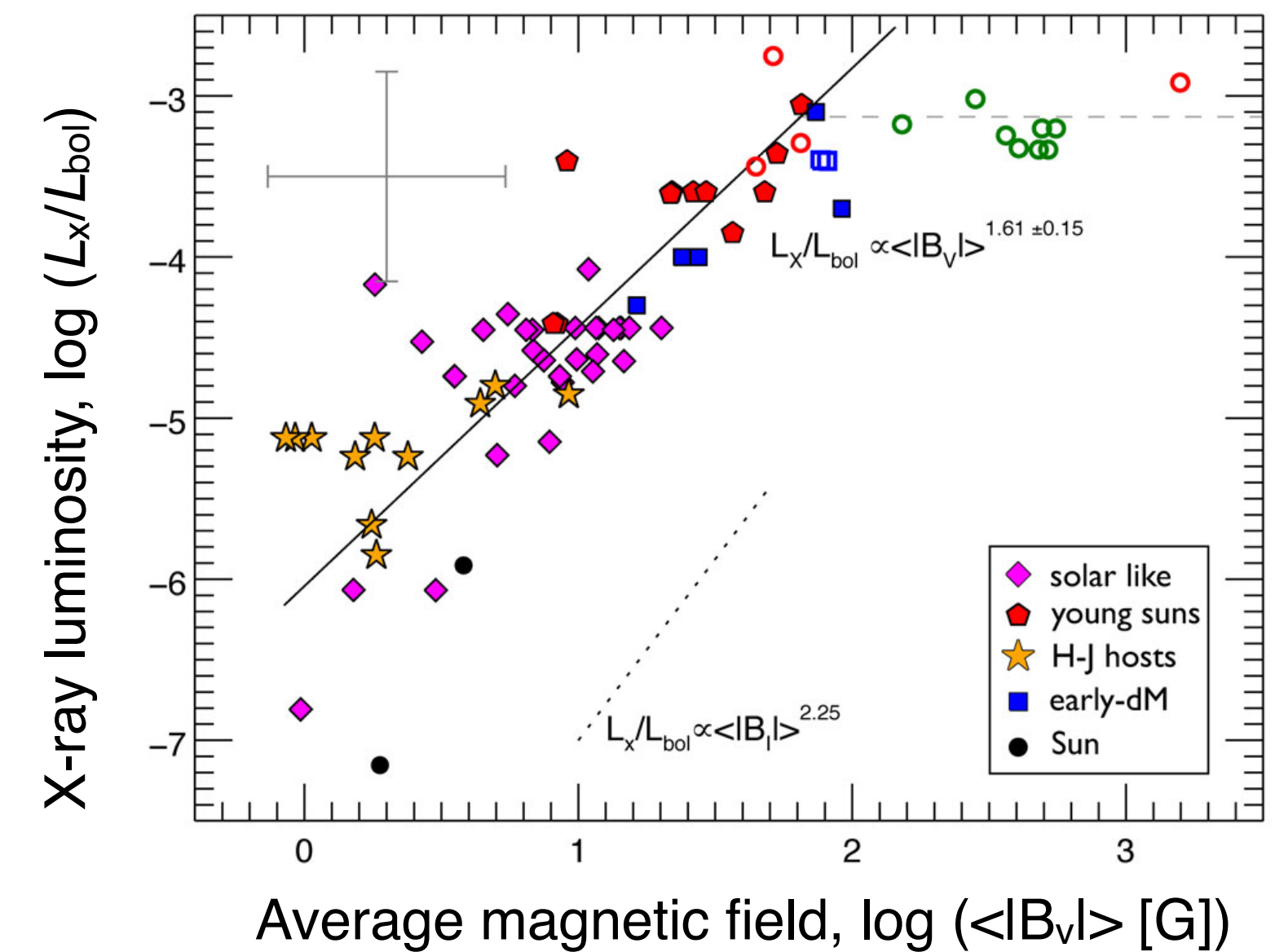
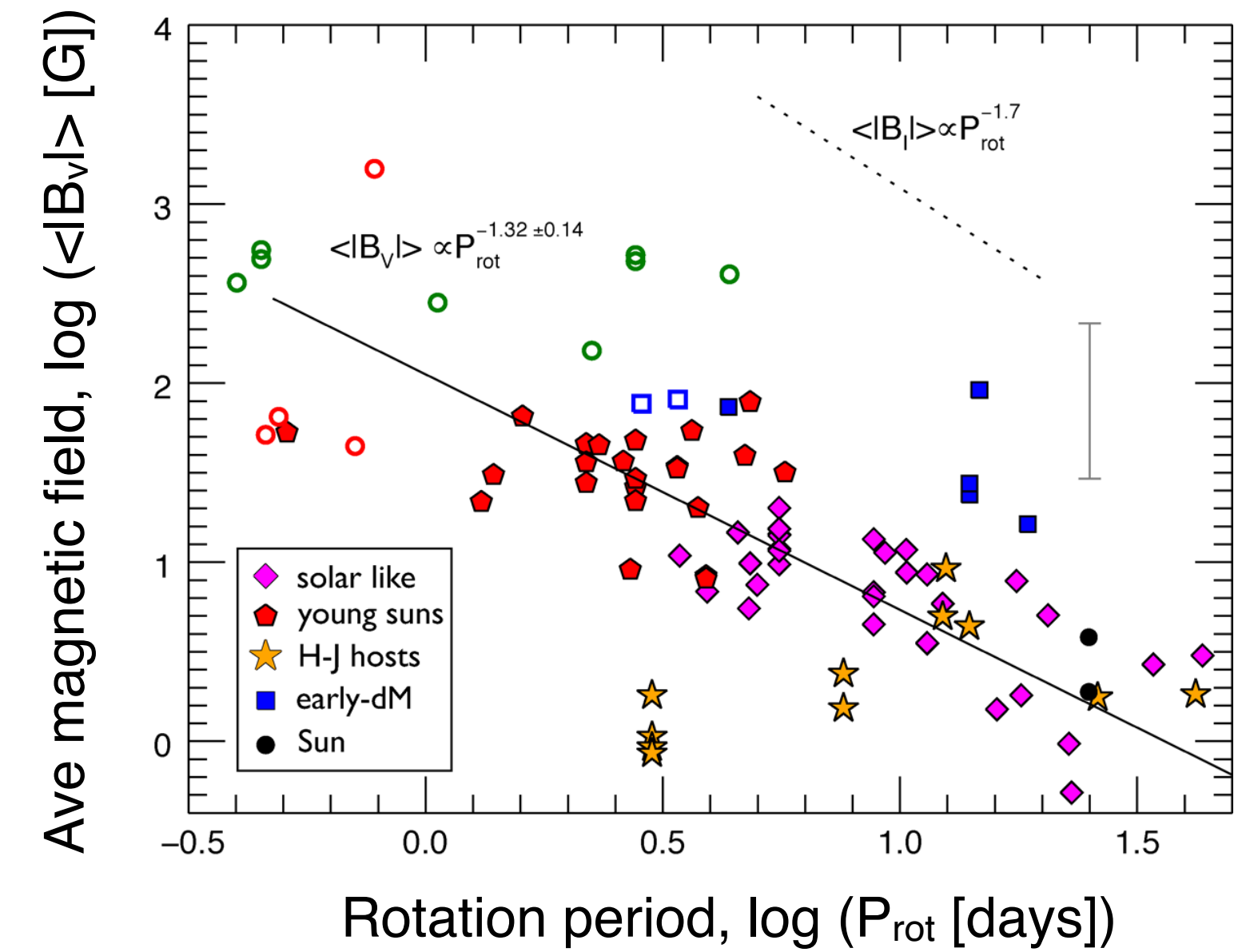
Some importance of Sun-as-a-star studies

- On solar-like stars...

Rotation speed — Mag field strength — X-ray luminosity

(\equiv Rossby number) (\equiv Total mag flux)

show strong correlations¹



[1: Skumanich 1972; Pizzolato+ 2003; Wright+ 2011; Vidotto+ 2014]

[Vidotto+ 2014]

1. Introduction

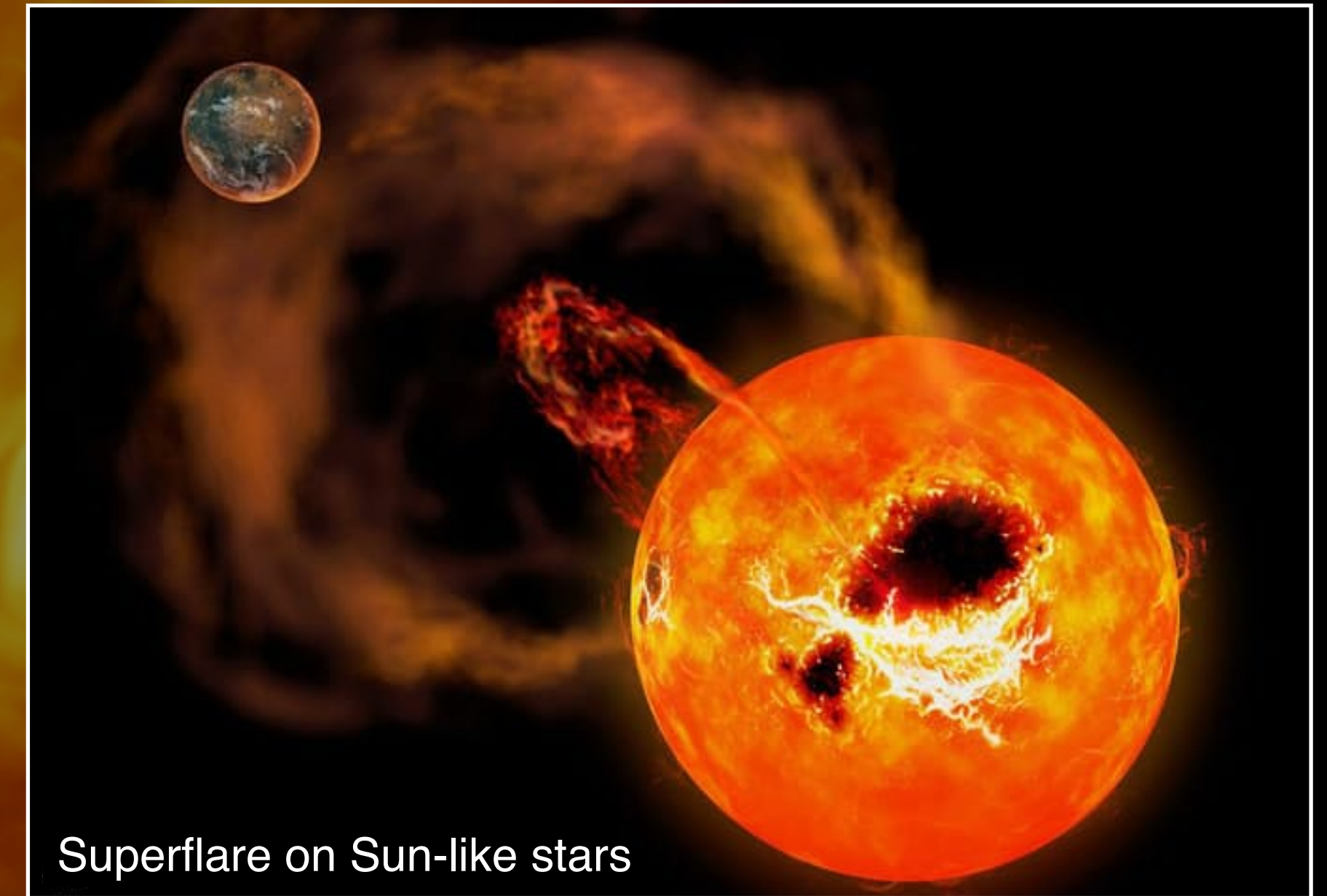
Some importance of Sun-as-a-star studies

- On solar-like stars...
 - Rotation speed** — **Mag field strength** — **X-ray luminosity**
(\equiv Rossby number) (\equiv Total mag flux)
- show strong correlations¹

Flares & CMEs: Giant sunspots, huge flares and CMEs



How can we characterize stellar active regions?



Superflare on Sun-like stars

1. Introduction

Some importance of Sun-as-a-star studies

- On solar-like stars...

Rotation speed — Mag field strength — X-ray luminosity

(\equiv Rossby number)

(\equiv Total mag flux)

show strong correlations¹

Flares & CMEs: Giant sunspots, huge flares and CMEs



How can we characterize stellar active regions?

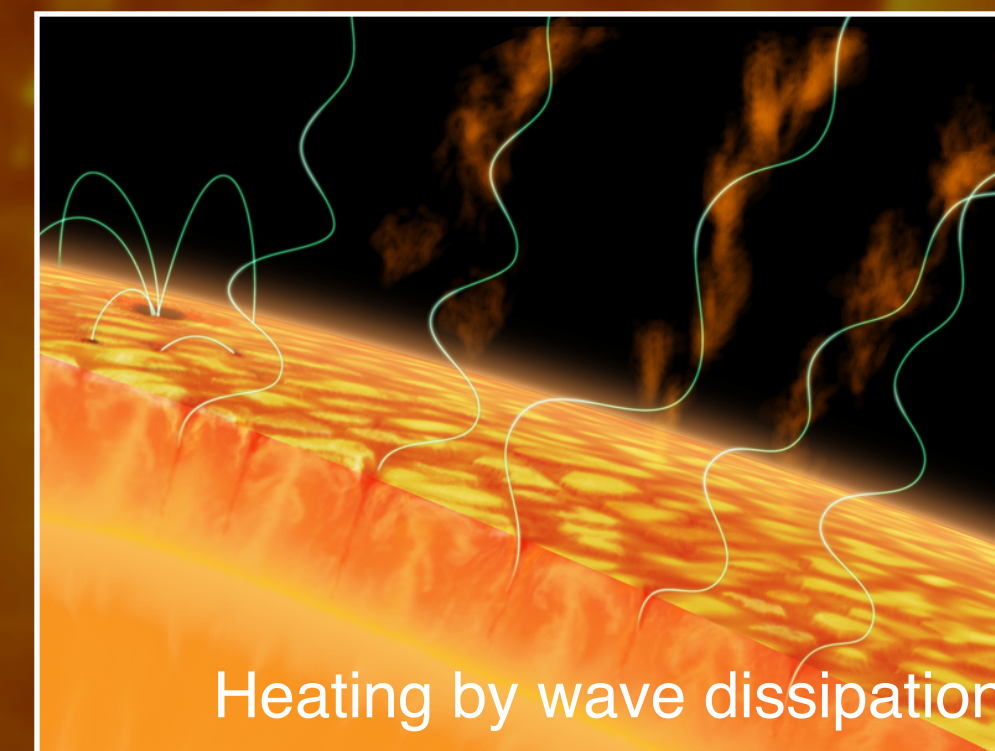
Extremely hot atmospheres: Strong XUV emission and winds



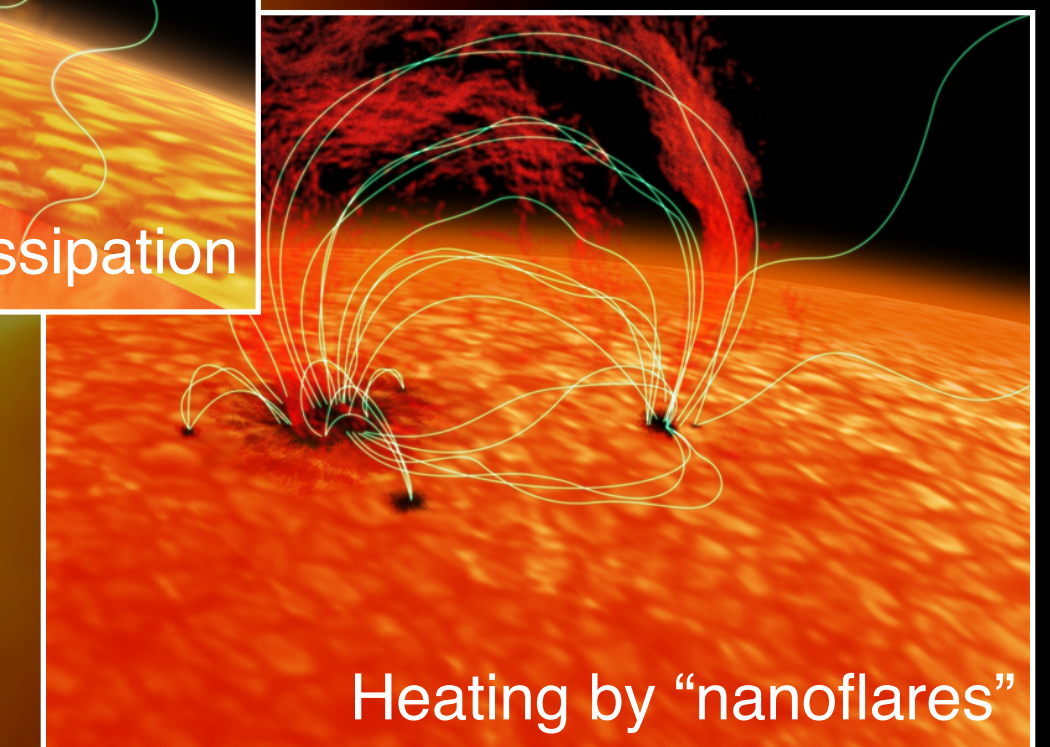
Do solar-like stars share common heating mechanism?



Superflare on Sun-like stars



Heating by wave dissipation



Heating by "nanoflares"







2. Characterization of Stellar ARs

THE ASTROPHYSICAL JOURNAL, 902:36 (15pp), 2020 October 10
 © 2020. The American Astronomical Society. All rights reserved.

<https://doi.org/10.3847/1538-4357/abadf9>



Sun-as-a-star Spectral Irradiance Observations of Transiting Active Regions

Shin Toriumi¹ , Vladimir S. Airapetian^{2,3} , Hugh S. Hudson^{4,5} , Carolus J. Schrijver⁶ , Mark C. M. Cheung⁶ , and
 Marc L. DeRosa⁶ 

¹ Institute of Space and Astronautical Science, Japan Aerospace Exploration Agency, 3-1-1 Yoshinodai, Chuo-ku, Sagami-hara, Kanagawa 252-5210, Japan
toriumi.shin@jaxa.jp

² Sellers Exoplanetary Environments Collaboration, NASA Goddard Space Flight Center, Greenbelt, MD, USA

³ Department of Physics, American University, Washington, DC, USA

⁴ School of Physics and Astronomy, University of Glasgow, Glasgow, UK

⁵ Space Sciences Laboratory, University of California at Berkeley, Berkeley, CA, USA

⁶ Lockheed Martin Solar and Astrophysics Laboratory, 3251 Hanover Street, Building/252, Palo Alto, CA 94304, USA

Received 2020 June 23; revised 2020 August 7; accepted 2020 August 9; published 2020 October 8

Abstract

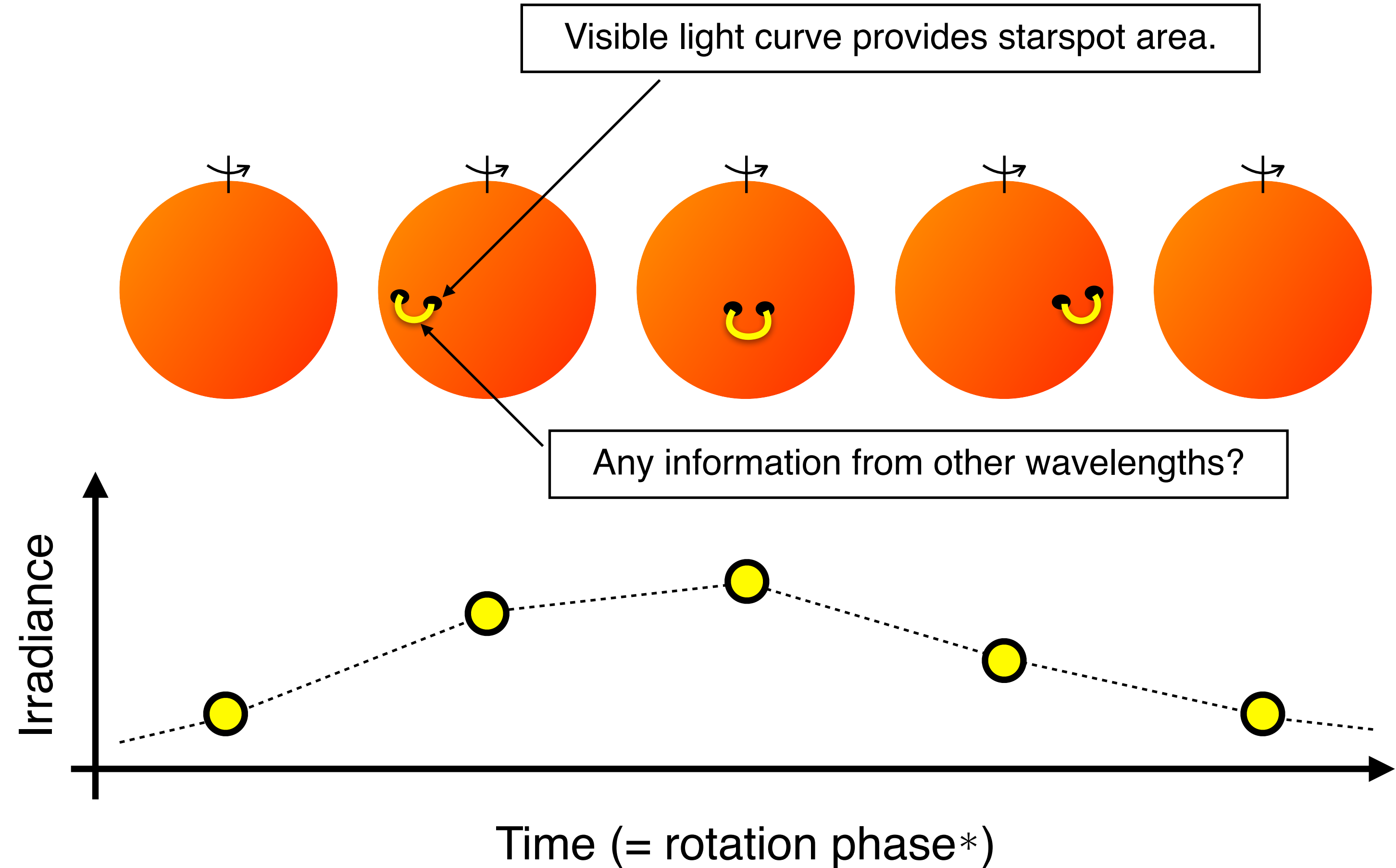
Major solar flares are prone to occur in active-region (AR) atmospheres associated with large, complex, dynamically evolving sunspots. This points to the importance of monitoring the evolution of starspots, not only in visible but also in ultraviolet (UV) and X-rays, in understanding the origin and occurrence of stellar flares. To this end, we perform spectral irradiance analysis on different types of transiting solar ARs by using a variety of full-disk synoptic observations. The target events are an isolated sunspot, spotless plage, and emerging flux in prolonged quiet-Sun conditions selected from the past decade. We find that the visible continuum and total solar irradiance become darkened when the spot is at the central meridian, whereas it is bright near the solar limb; UV bands sensitive to the chromosphere correlate well with the variation of total unsigned magnetic flux in the photosphere; amplitudes of extreme ultraviolet (EUV) and soft X-ray increase with the characteristic temperature, whose light curves are flat-topped due to their sensitivity to the optically thin corona; the transiting spotless plage does not show the darkening in the visible irradiance, while the emerging flux produces an asymmetry in all light curves about the central meridian. The multiwavelength Sun-as-a-star study described here indicates that the time lags between the coronal and photospheric light curves have the potential to probe the extent of coronal magnetic fields above the starspots. In addition, EUV wavelengths that are sensitive to temperatures just below 1 MK sometimes show antiphased variations, which may be used for diagnosing plasmas around starspots.

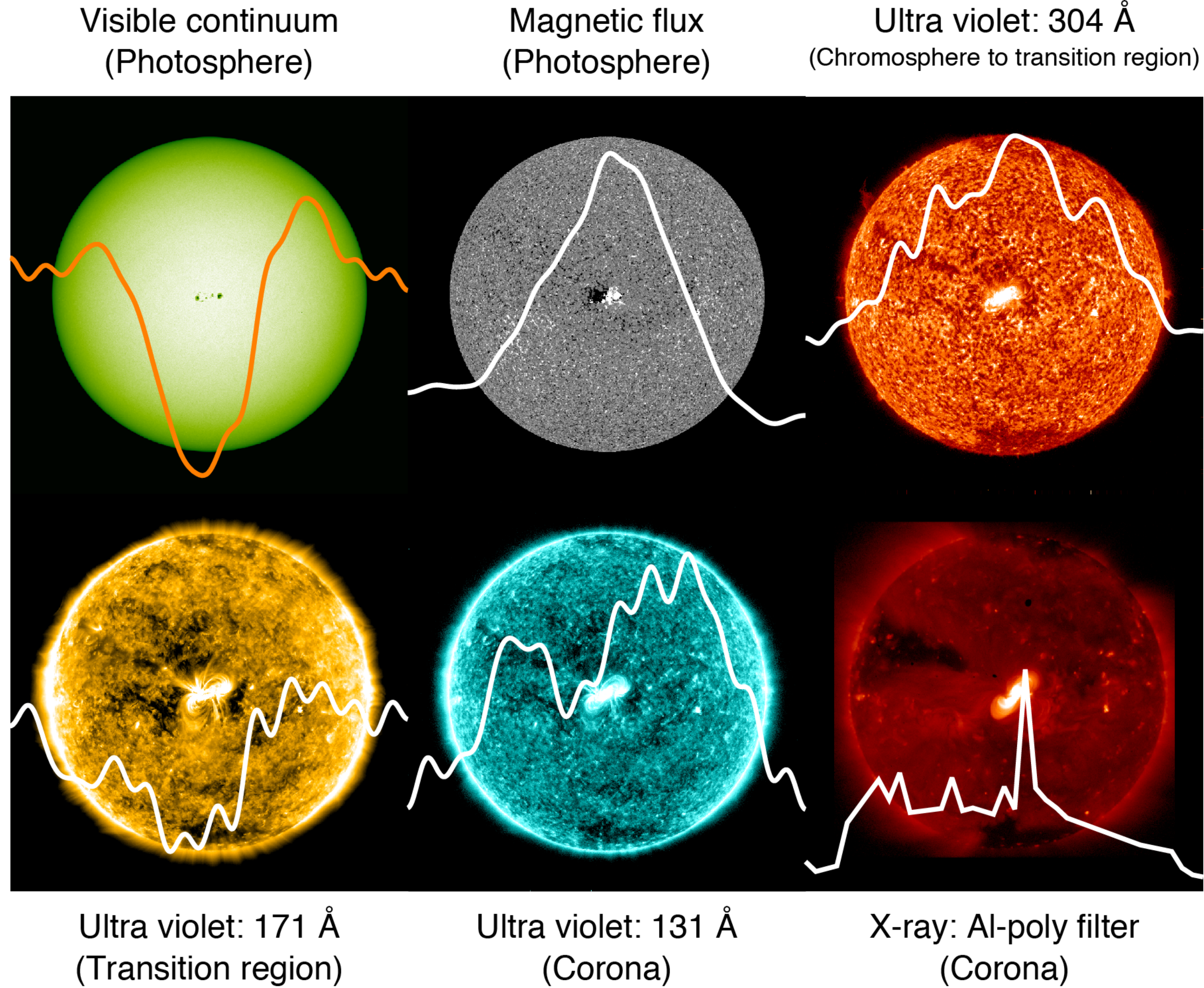
Unified Astronomy Thesaurus concepts: [Solar spectral irradiance \(1501\)](#); [Sunspots \(1653\)](#); [Solar active regions \(1974\)](#); [Solar flares \(1496\)](#); [Solar analogs \(1941\)](#); [Starspots \(1572\)](#); [Stellar flares \(1603\)](#); [Time domain astronomy \(2109\)](#)

Supporting material: animations

2. Characterization of Stellar ARs

- Sun-as-a-star light curves
 - Monitor starspots **not only in visible but also in UV and X-rays** to track atmospheric evolution
 - Test this possibility using solar data
 - Plot full-disk light curves in various wavelengths when **only a single sunspot group transits** across the solar disk in prolonged quiet-Sun conditions
 - Instruments
 - ▶ SDO/HMI: visible imaging, magnetic fields
 - ▶ SDO/AIA: UV and EUV imaging
 - ▶ Hinode/XRT: soft X-ray imaging
 - ▶ GOES/XRS: soft X-ray (no spatial res)
 - ▶ SORCE/TIM: total solar irradiance (no spatial res)
 - 14 wavelengths in total





Visible continuum
(Photosphere)

Magnetic flux
(Photosphere)

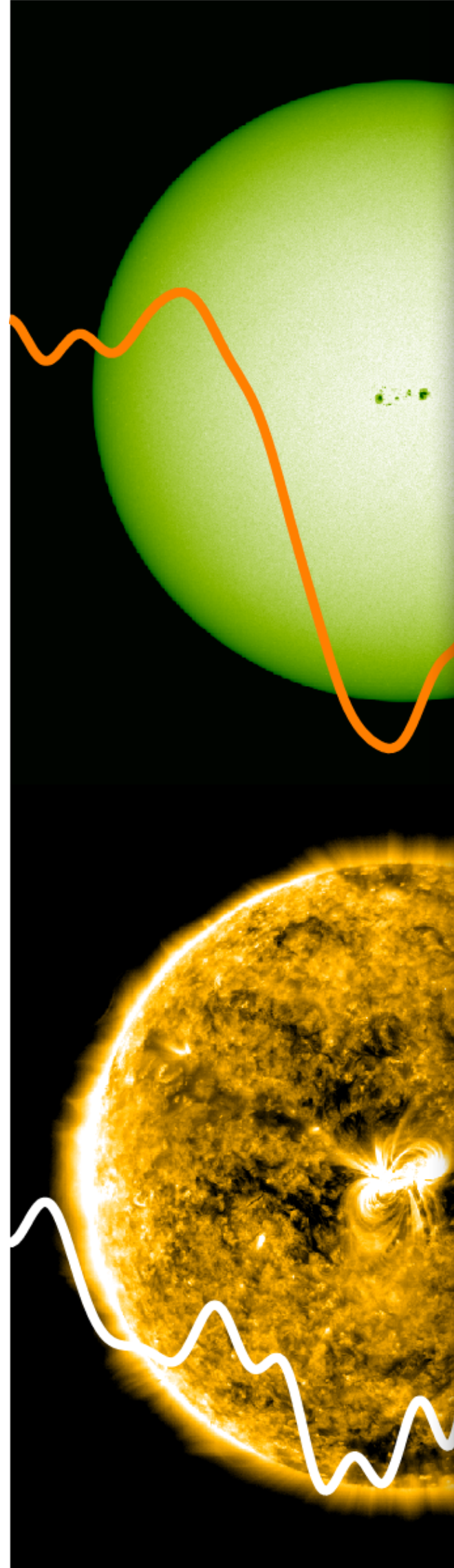
Ultra violet: 304 Å
(Chromosphere to transition region)

Ultra violet: 171 Å
(Transition region)

Ultra violet: 131 Å
(Corona)

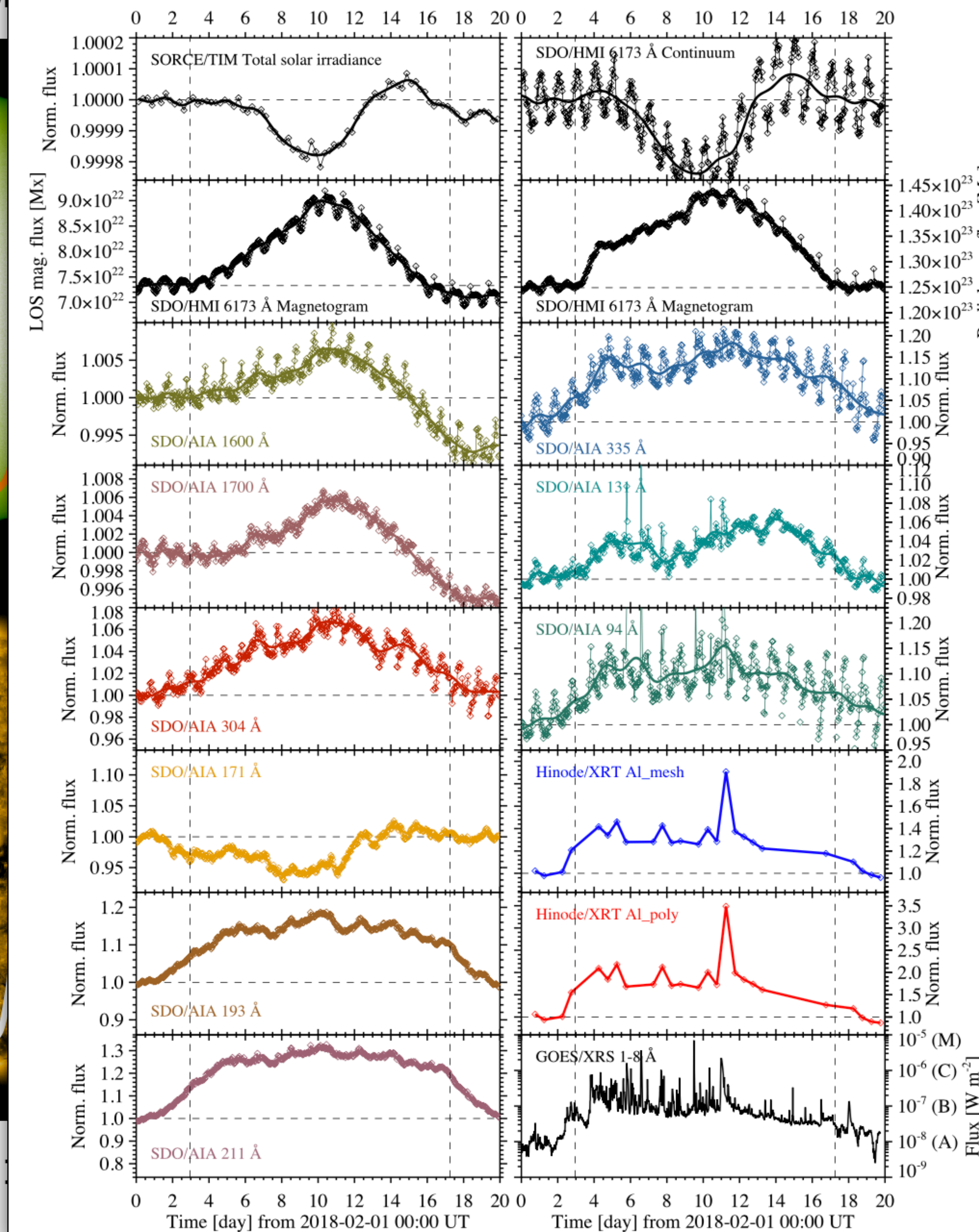
X-ray: Al-poly filter
(Corona)

Visible continuum
(Photosphere)

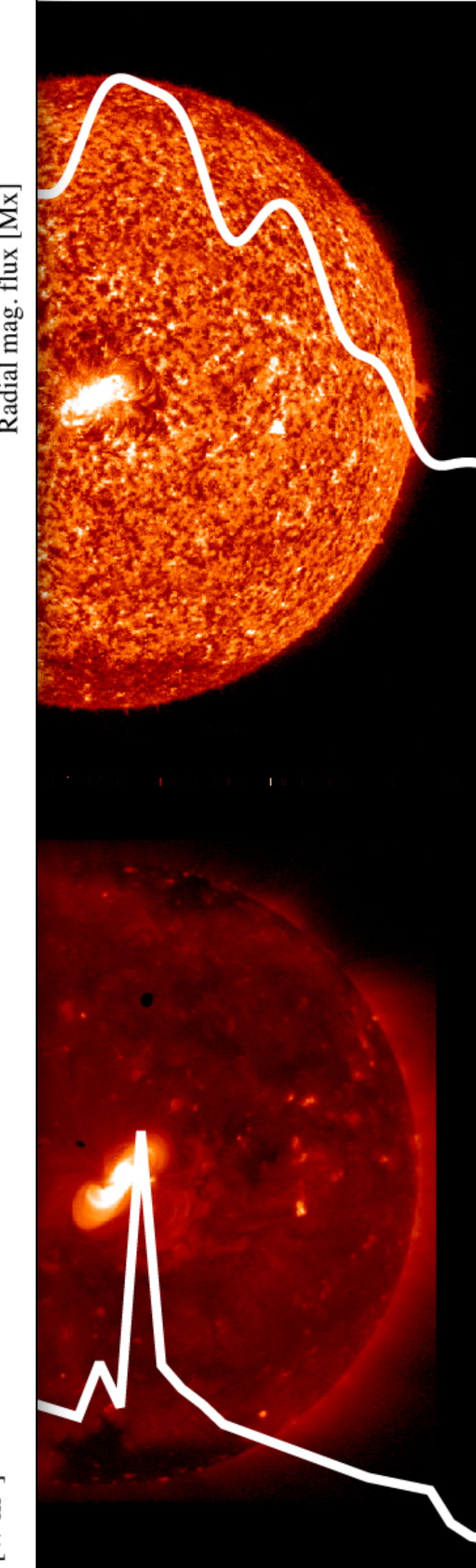


Ultra violet
(Transition region)

Magnetic flux
Sunspot: AR 12699



Ultra violet: 304 Å
(Transition region to corona)

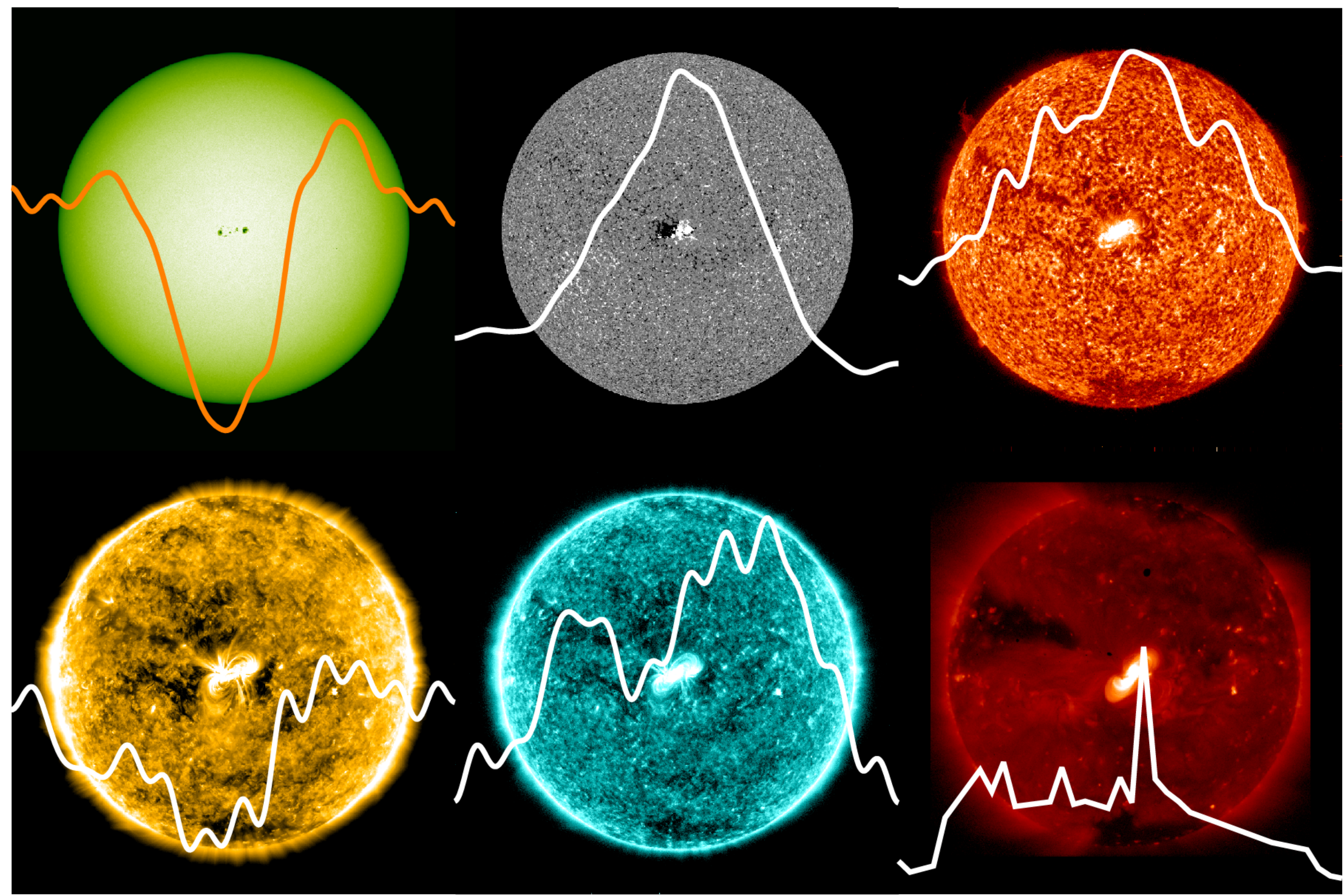


Al-poly filter
(Corona)

Visible continuum
(Photosphere)

Magnetic flux
(Photosphere)

Ultra violet: 304 Å
(Chromosphere to transition region)



Ultra violet: 171 Å
(Transition region)

Ultra violet: 131 Å
(Corona)

X-ray: Al-poly filter
(Corona)

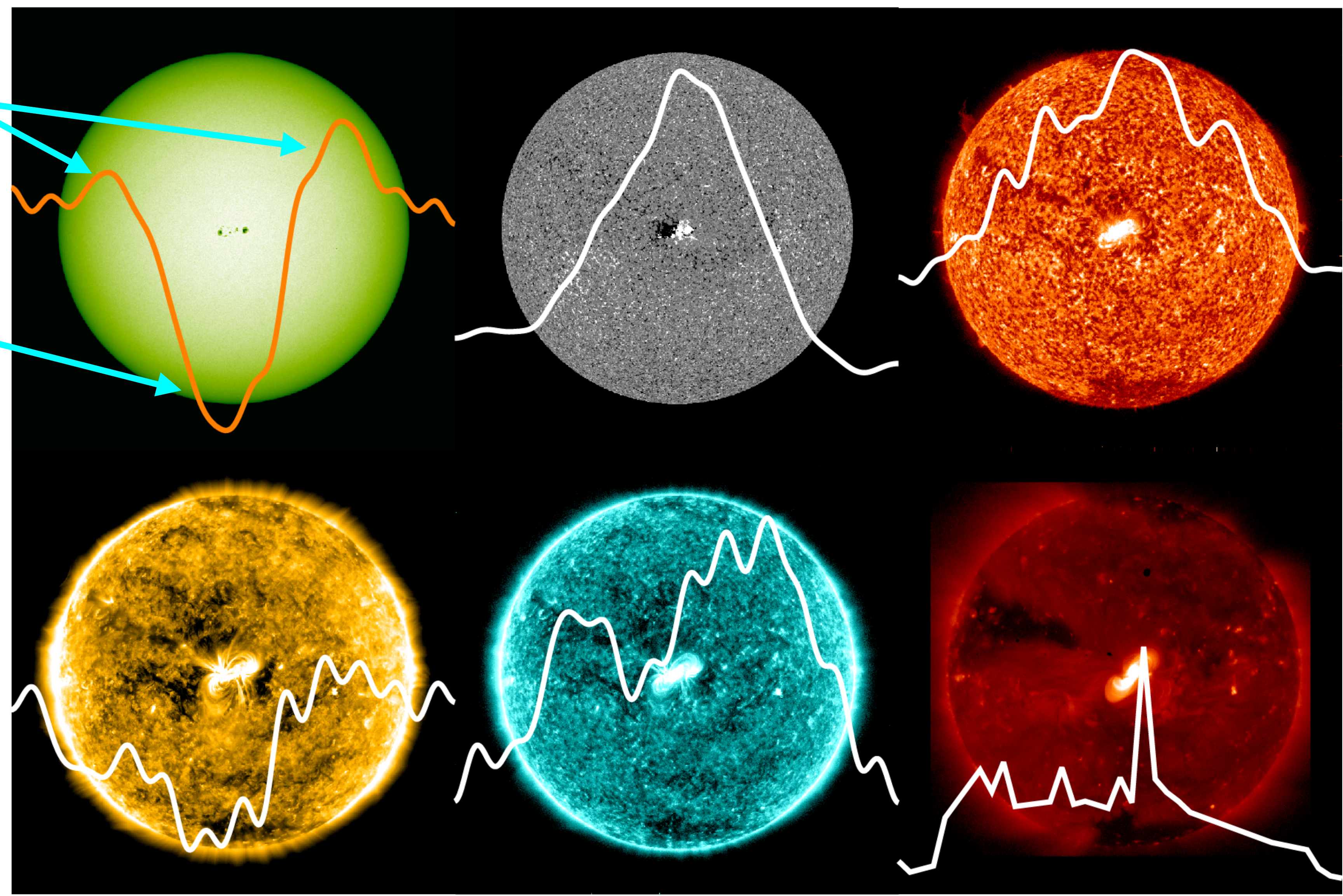
Visible continuum
(Photosphere)

Magnetic flux
(Photosphere)

Ultra violet: 304 Å
(Chromosphere to transition region)

“Shoulders”: faculae
are dominant

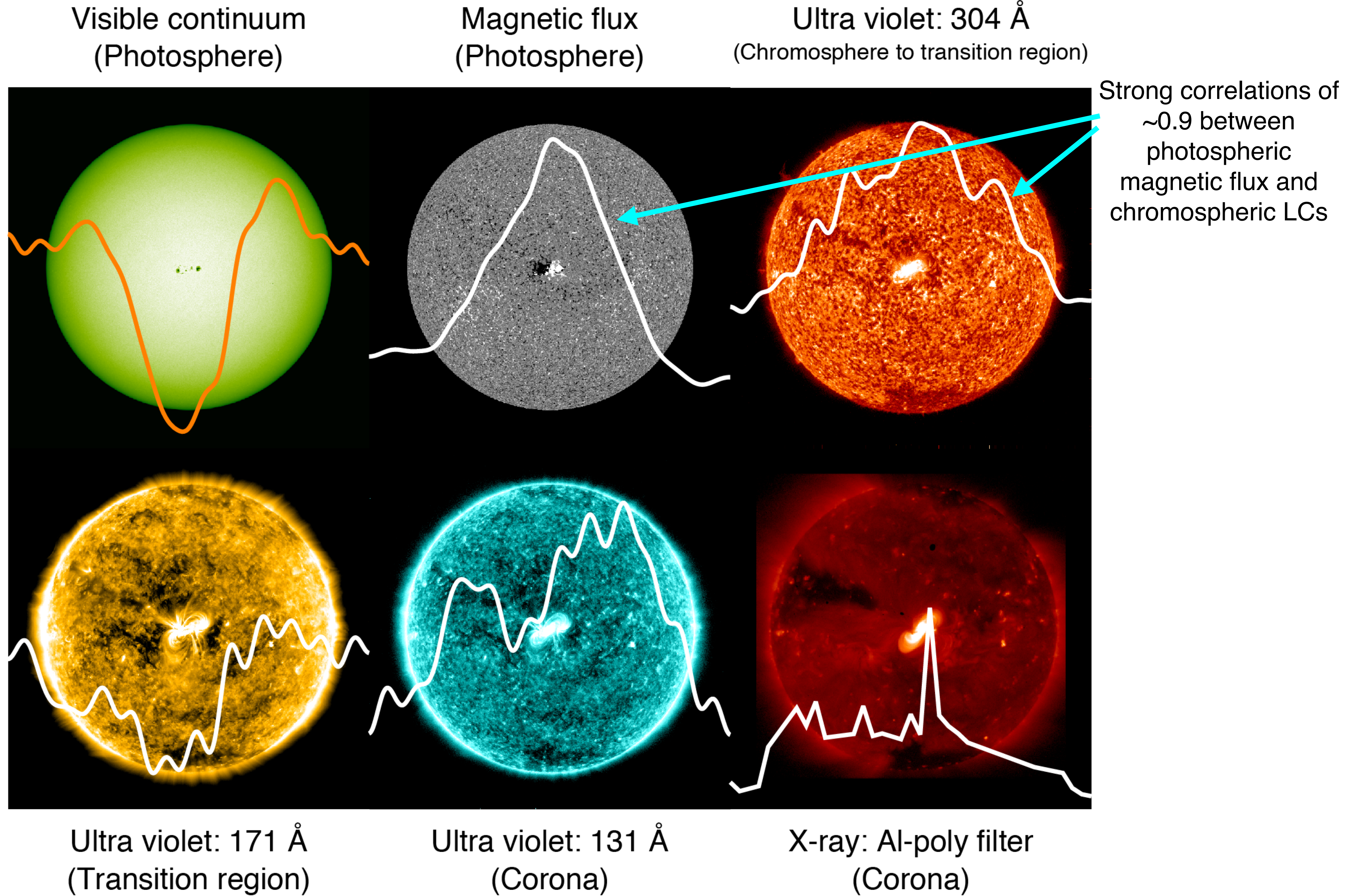
“Dip”: sunspot is dark

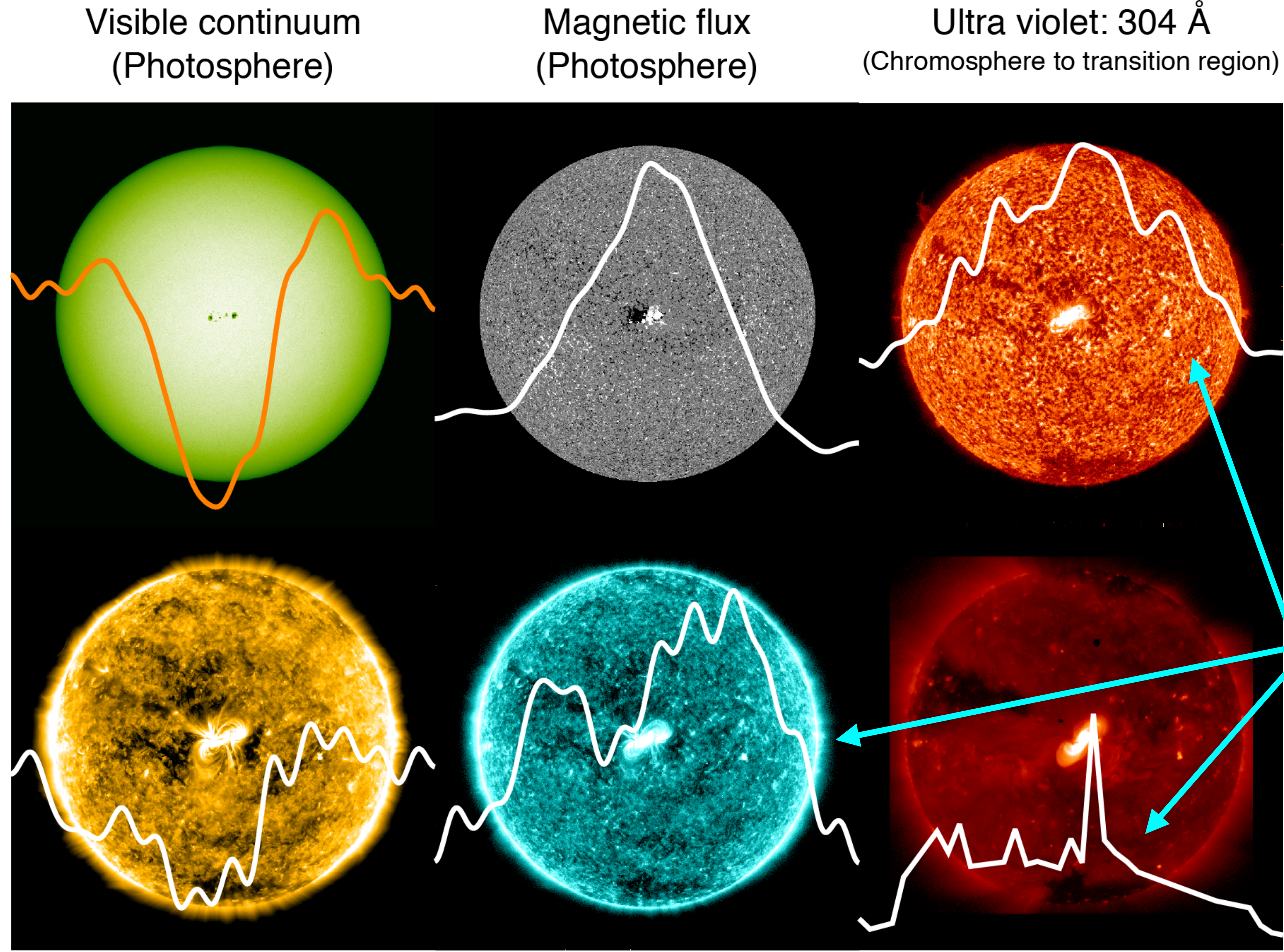


Ultra violet: 171 Å
(Transition region)

Ultra violet: 131 Å
(Corona)

X-ray: Al-poly filter
(Corona)





Visible continuum
(Photosphere)

Magnetic flux
(Photosphere)

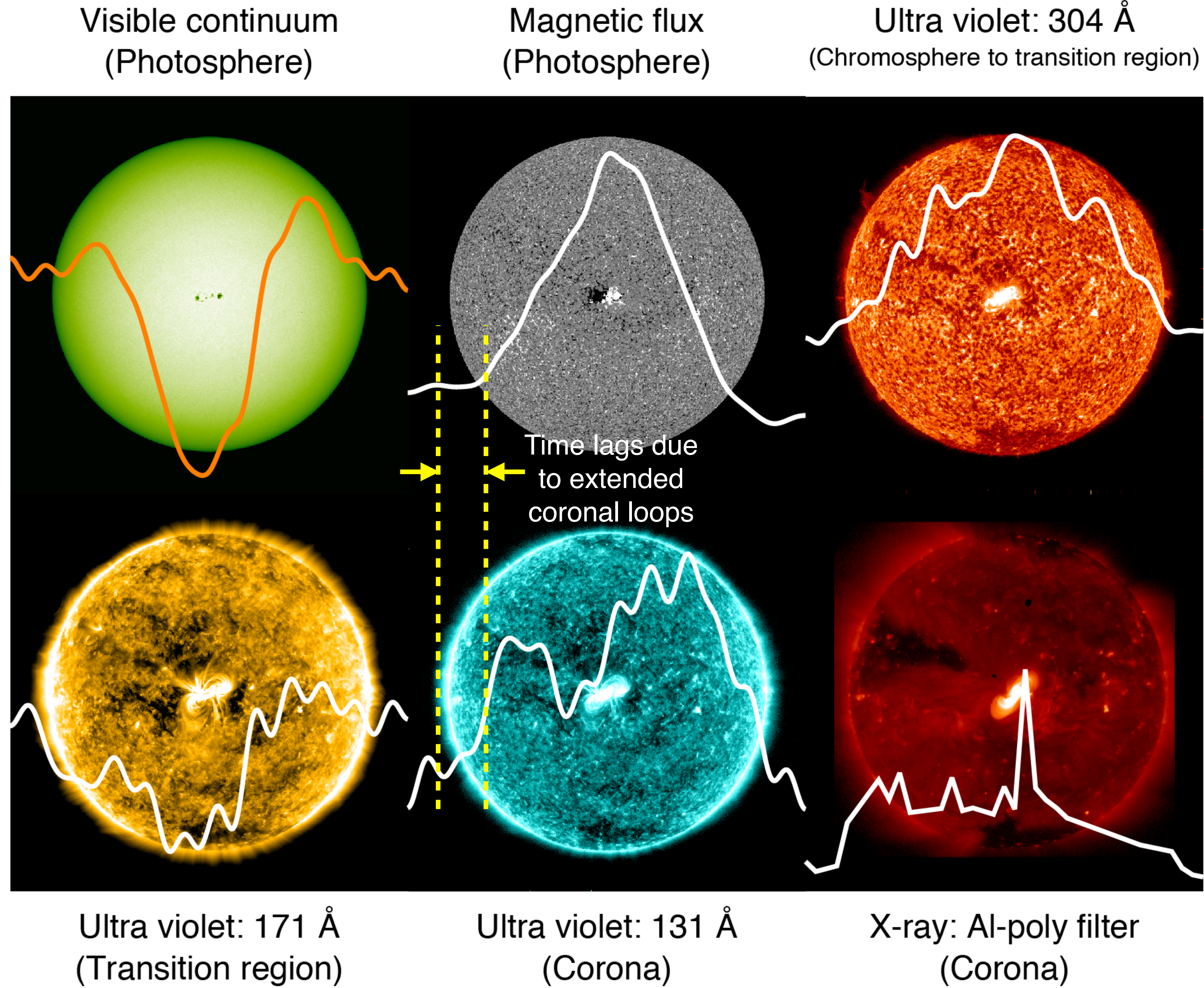
Ultra violet: 304 Å
(Chromosphere to transition region)

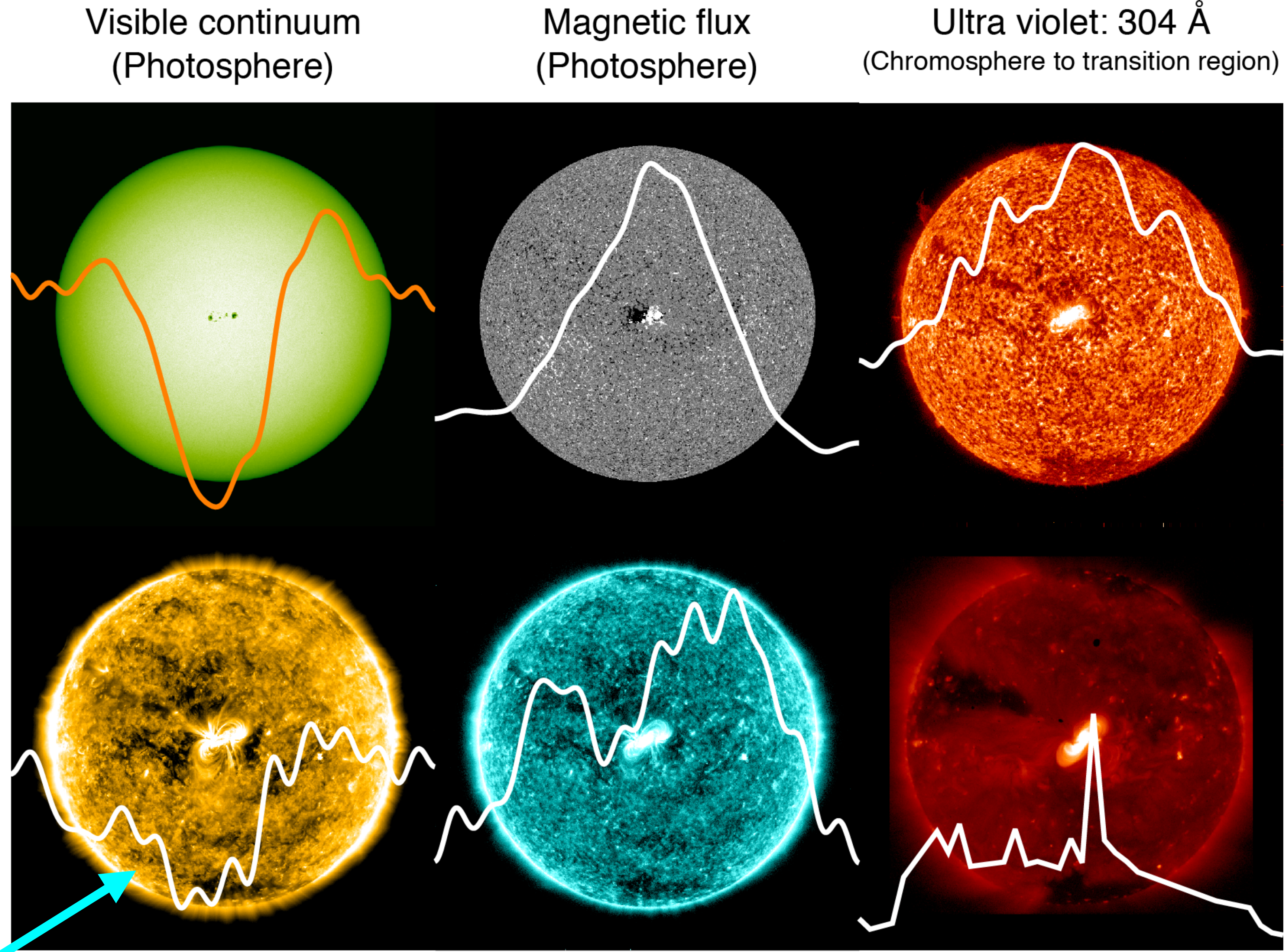
Ultra violet: 171 Å
(Transition region)

Ultra violet: 131 Å
(Corona)

X-ray: Al-poly filter
(Corona)

UV and X-rays:
amplitude increases
with temperature





Visible continuum
(Photosphere)

Magnetic flux
(Photosphere)

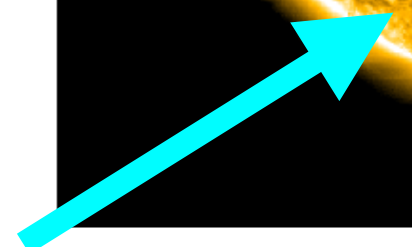
Ultra violet: 304 Å
(Chromosphere to transition region)

Ultra violet: 171 Å
(Transition region)

Ultra violet: 131 Å
(Corona)

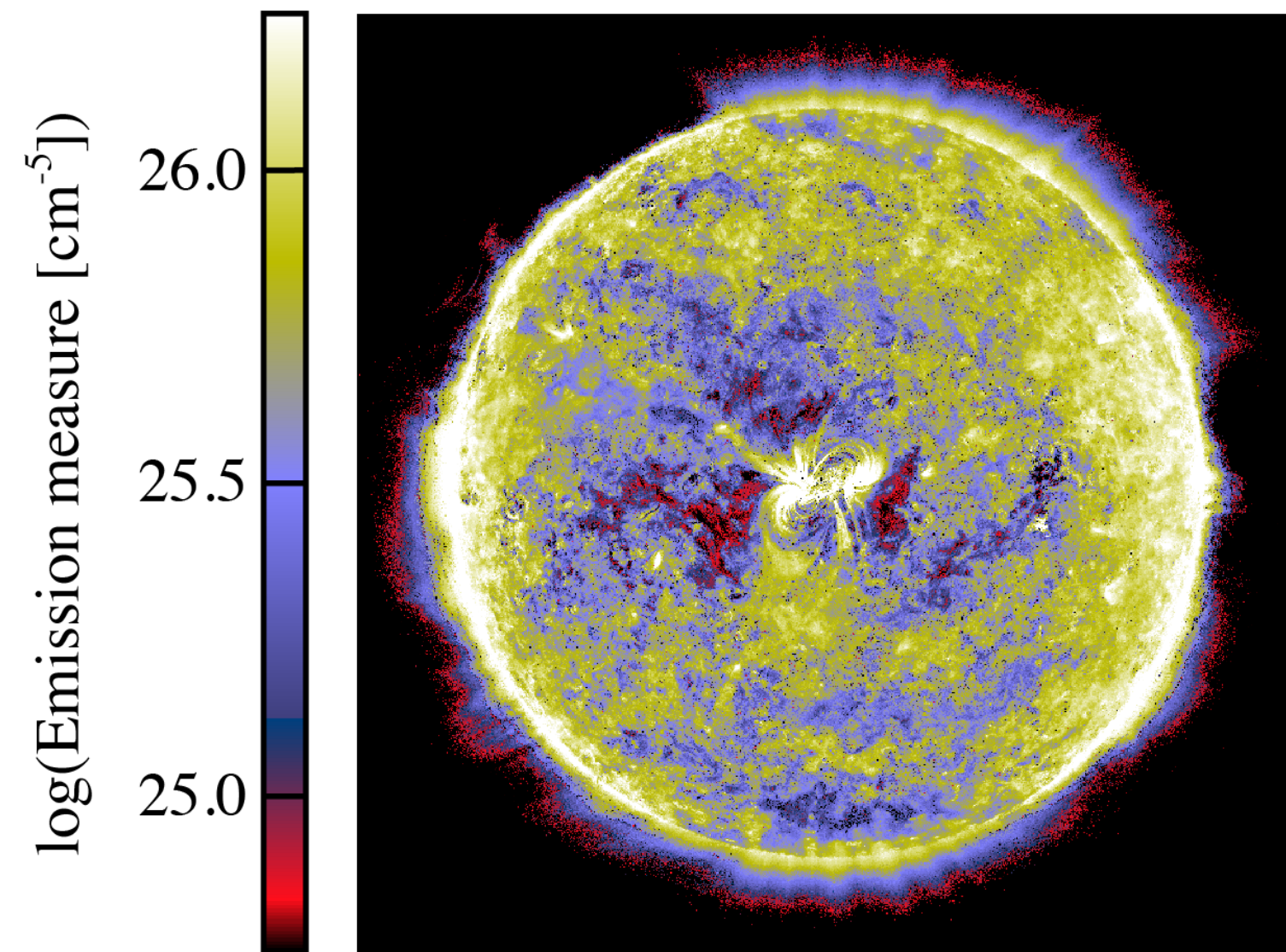
X-ray: Al-poly filter
(Corona)

WHAT'S THIS?

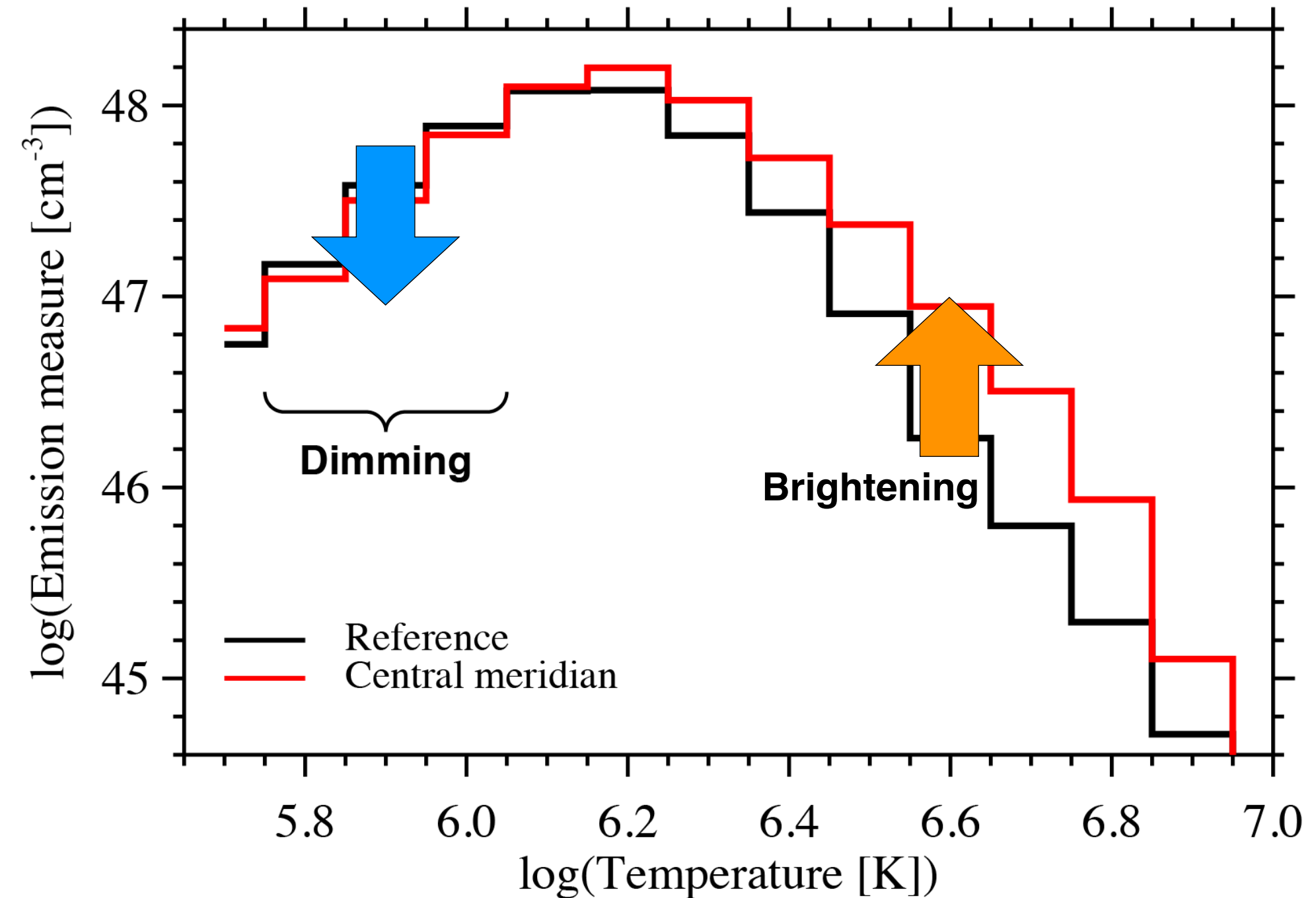


2. Characterization of Stellar ARs

- Differential Emission Measure inversion: $EM = \int n_e^2 dV$
 - Emission measure as a function of temperature



Emission measure: $\log T = [5.75, 6.05]$



- ▶ EM of TR temperatures (0.6-0.8 MK) is reduced over a wide area around AR
- ▶ EM of coronal temperatures (>1.5 MK) is all increased

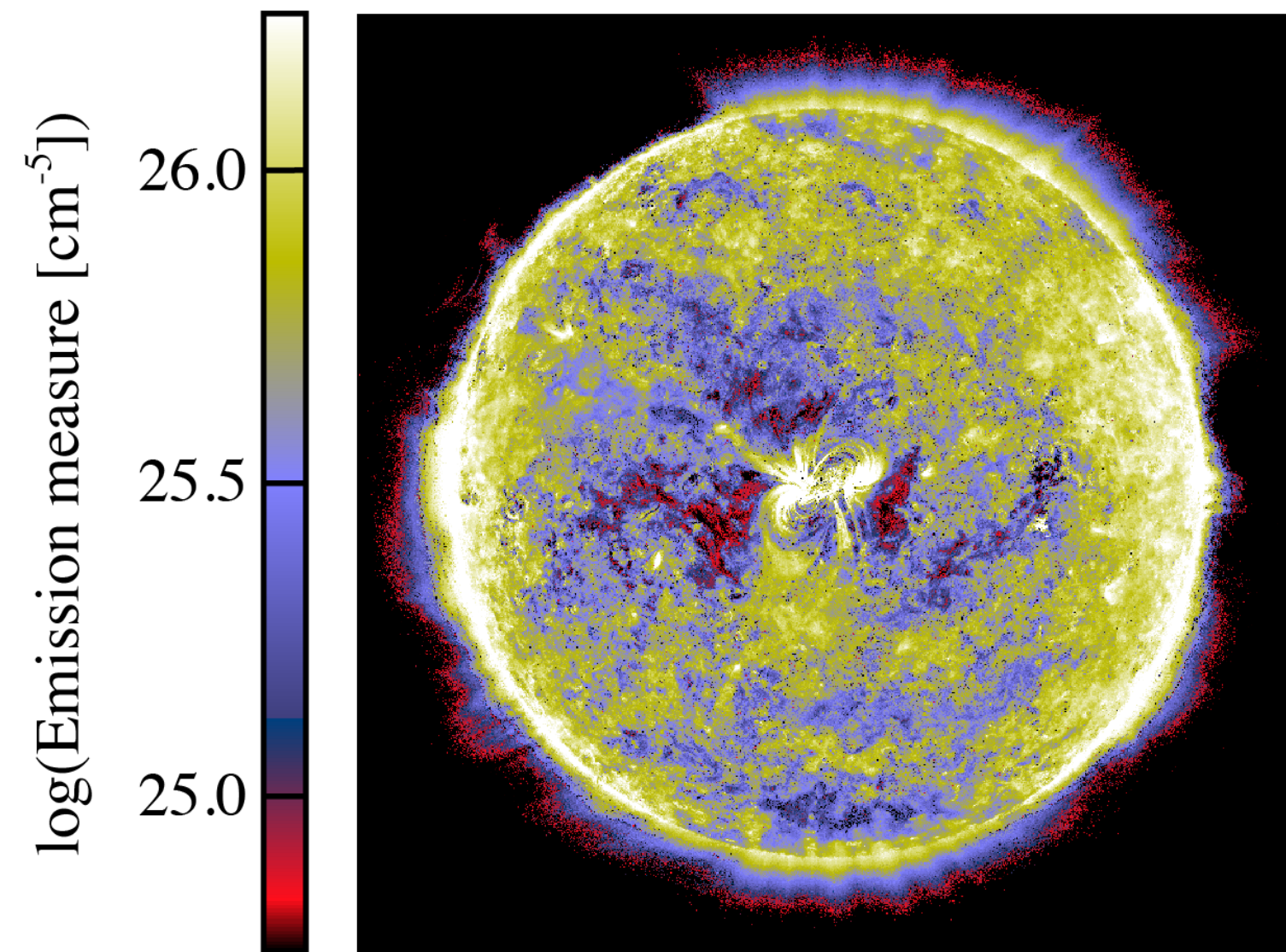
→ **Significant heating of plasma, probably owing to AR, over ~40% of the solar disk over ~10 days**

See also

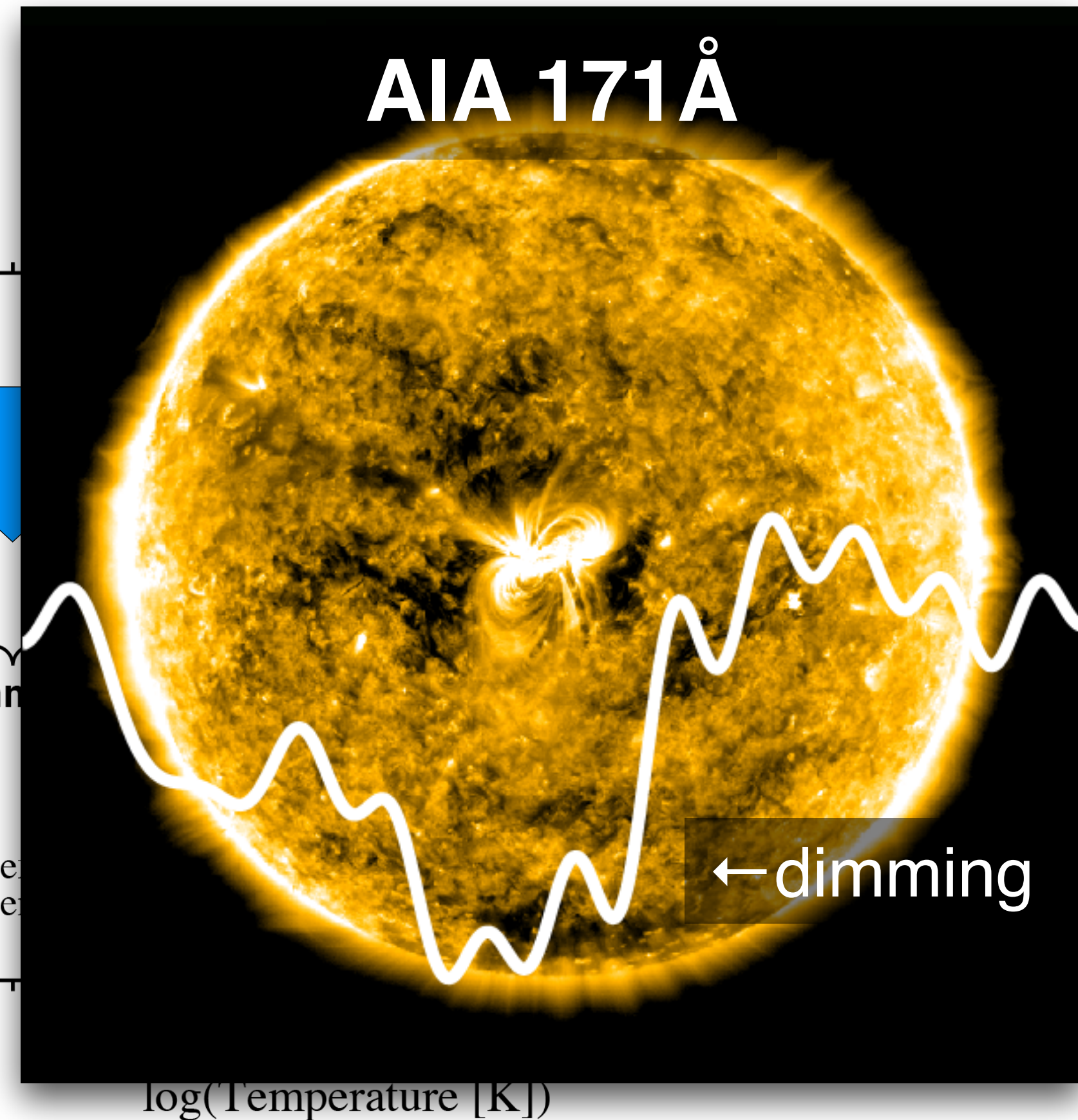
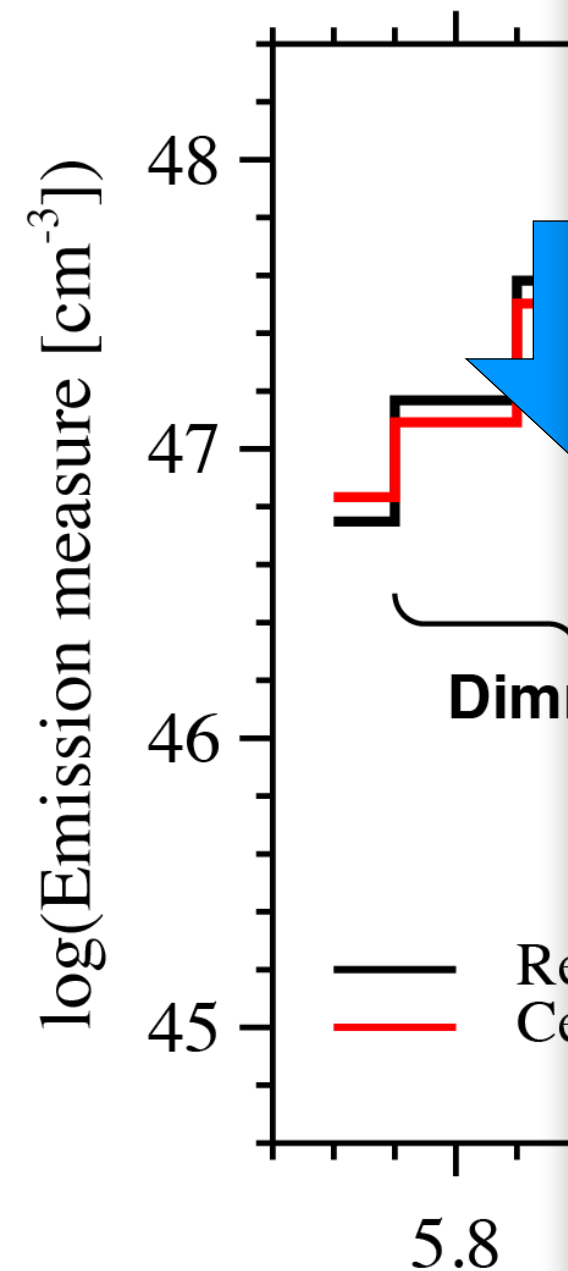
- Kazachenko & Hudson (2020)
- Singh, Sterling, & Moore (2021)
- Payne & Sun (2021)

2. Characterization of Stellar ARs

- Differential Emission Measure inversion: $EM = \int n_e^2 dV$
 - Emission measure as a function of temperature



Emission measure: $\log T = [5.75, 6.05]$



- ▶ EM of TR temperatures (0.6-0.8 MK) is reduced over a wide area around AR
- ▶ EM of coronal temperatures (>1.5 MK) is all increased

→ **Significant heating of plasma, probably owing to AR, over ~40% of the solar disk over ~10 days**

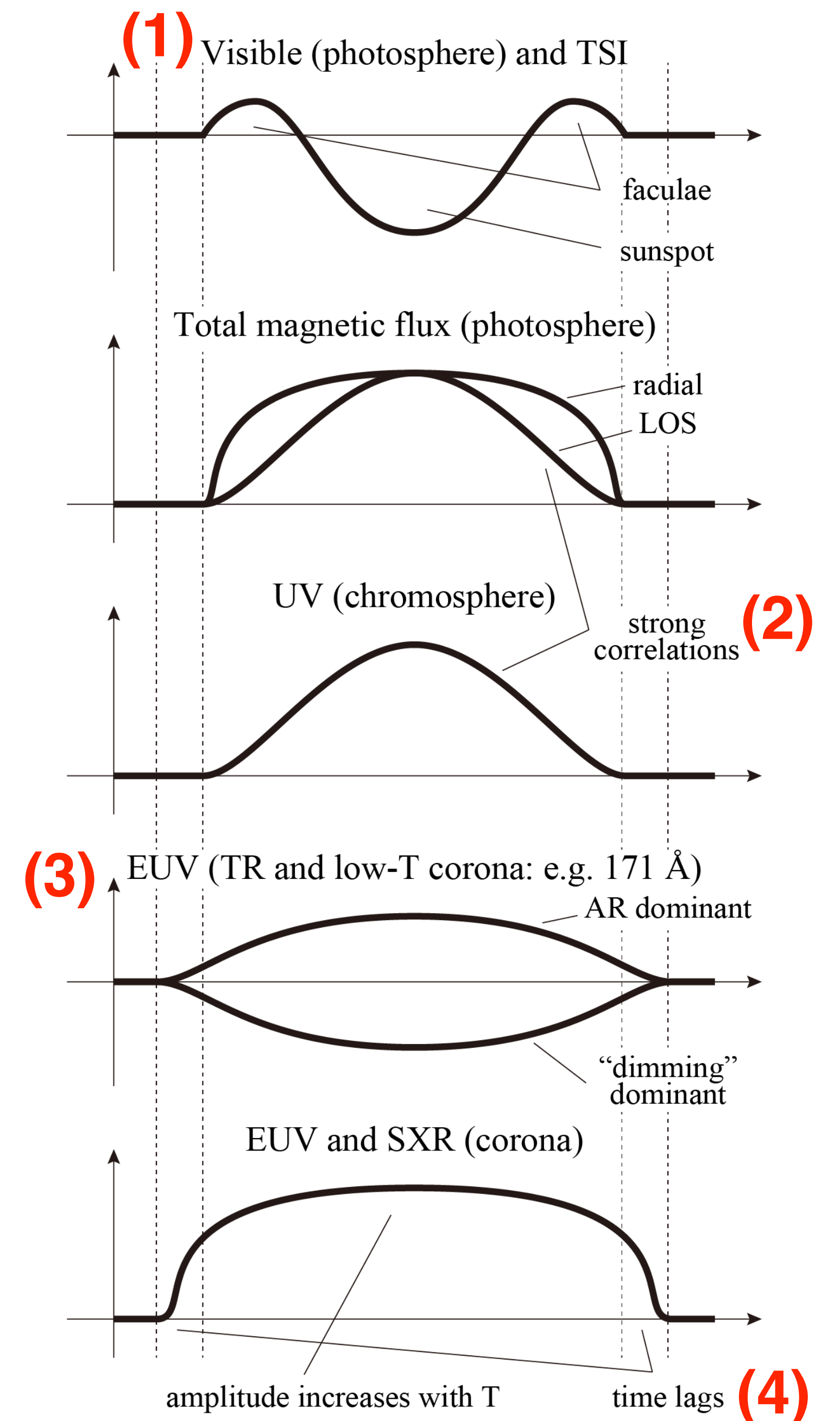
See also

- Kazachenko & Hudson (2020)
- Singh, Sterling, & Moore (2021)
- Payne & Sun (2021)

2. Characterization of Stellar ARs

- Possible “tools” for diagnosing stellar ARs
 - (1) **Visible** for starspot size and evolution
 - (2) **Near UV radiations** as the proxy for the total magnetic flux on the stellar surface (like Ca II monitoring)
 - (3) **Extreme UV sensitive to sub-MK** for diagnosing plasmas around starspots
 - (4) **Time lags between the coronal and photospheric curves** for the extension of coronal magnetic fields

Long-term, multi-wavelength monitoring of stars give us clues to understand AR evolutions



3. Universality of Atmospheric Heating

THE ASTROPHYSICAL JOURNAL, 927:179 (16pp), 2022 March 10

© 2022. The Author(s). Published by the American Astronomical Society.


OPEN ACCESS

<https://doi.org/10.3847/1538-4357/ac5179>



Universal Scaling Laws for Solar and Stellar Atmospheric Heating

Shin Toriumi¹  and Vladimir S. Airapetian^{2,3} 

¹ Institute of Space and Astronautical Science, Japan Aerospace Exploration Agency, 3-1-1 Yoshinodai, Chuo-ku, Sagami-hara, Kanagawa 252-5210, Japan 
toriumi.shin@jaxa.jp

² Sellers Exoplanetary Environments Collaboration, NASA Goddard Space Flight Center, Greenbelt, MD, USA

³ Department of Physics, American University, Washington, DC, USA

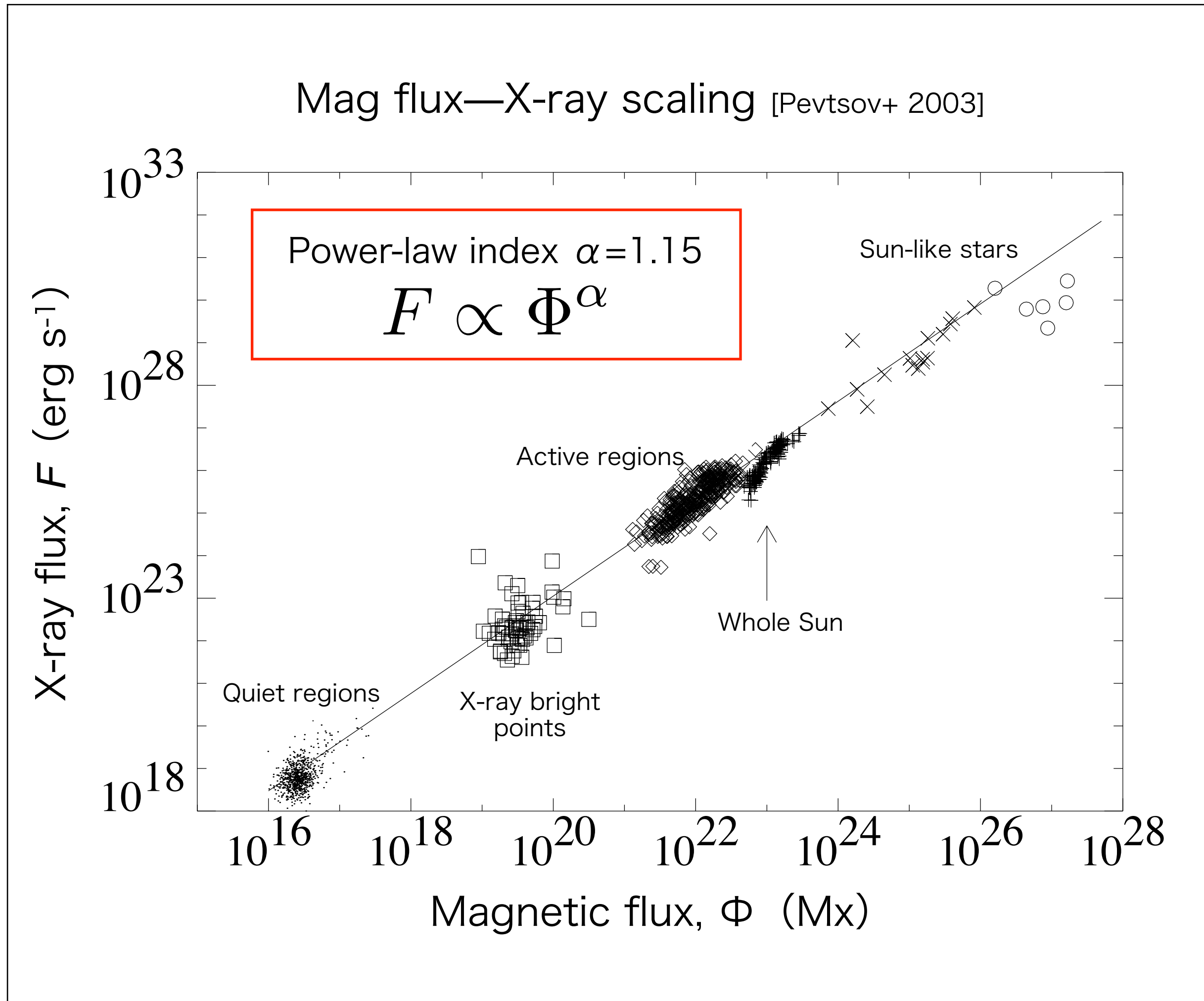
Received 2021 December 11; revised 2022 January 27; accepted 2022 February 1; published 2022 March 15

Abstract

The Sun and Sun-like stars commonly host multimillion-kelvin coronae and 10,000 K chromospheres. These extremely hot gases generate X-ray and extreme ultraviolet emissions that may impact the erosion and chemistry of (exo)planetary atmospheres, influencing the climate and conditions for habitability. However, the mechanism of coronal and chromospheric heating is still poorly understood. While the magnetic field most probably plays a key role in driving and transporting energy from the stellar surface upwards, it is not clear whether the atmospheric heating mechanisms of the Sun and active Sun-like stars can be described in a unified manner. To this end, we report on a systematic survey of the responses of solar and stellar atmospheres to surface magnetic flux over a wide range of temperatures. By analyzing 10 years of multiwavelength synoptic observations of the Sun, we reveal that the irradiance and magnetic flux show power-law relations with an exponent decreasing from above unity to below as the temperature decreases from the corona to the chromosphere. Moreover, this trend indicating the efficiency of atmospheric heating can be extended to Sun-like stars. We also discover that the power-law exponent depends on the solar cycle, becoming smallest at maximum activity, probably due to the saturation of atmospheric heating. Our study provides observational evidence that the mechanism of atmospheric heating is universal among the Sun and Sun-like stars, regardless of age or activity.

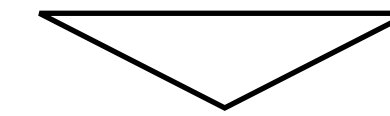
Unified Astronomy Thesaurus concepts: [G dwarf stars \(556\)](#); [Solar analogs \(1941\)](#); [Stellar coronae \(305\)](#); [Stellar chromospheres \(230\)](#); [Stellar magnetic fields \(1610\)](#); [Solar coronal heating \(1989\)](#); [Solar chromospheric heating \(1987\)](#); [Solar magnetic fields \(1503\)](#)

3. Universality of Atmospheric Heating



- Previous studies

- X-ray luminosity has a uniform scaling relationship with a power-law index of $\alpha \approx 1.15$
- One of the key results of JAXA's Yohkoh satellite
- Barometer for efficiency of coronal heating in regard to surface magnetic flux¹



- What about in other lines (= temperatures)?²

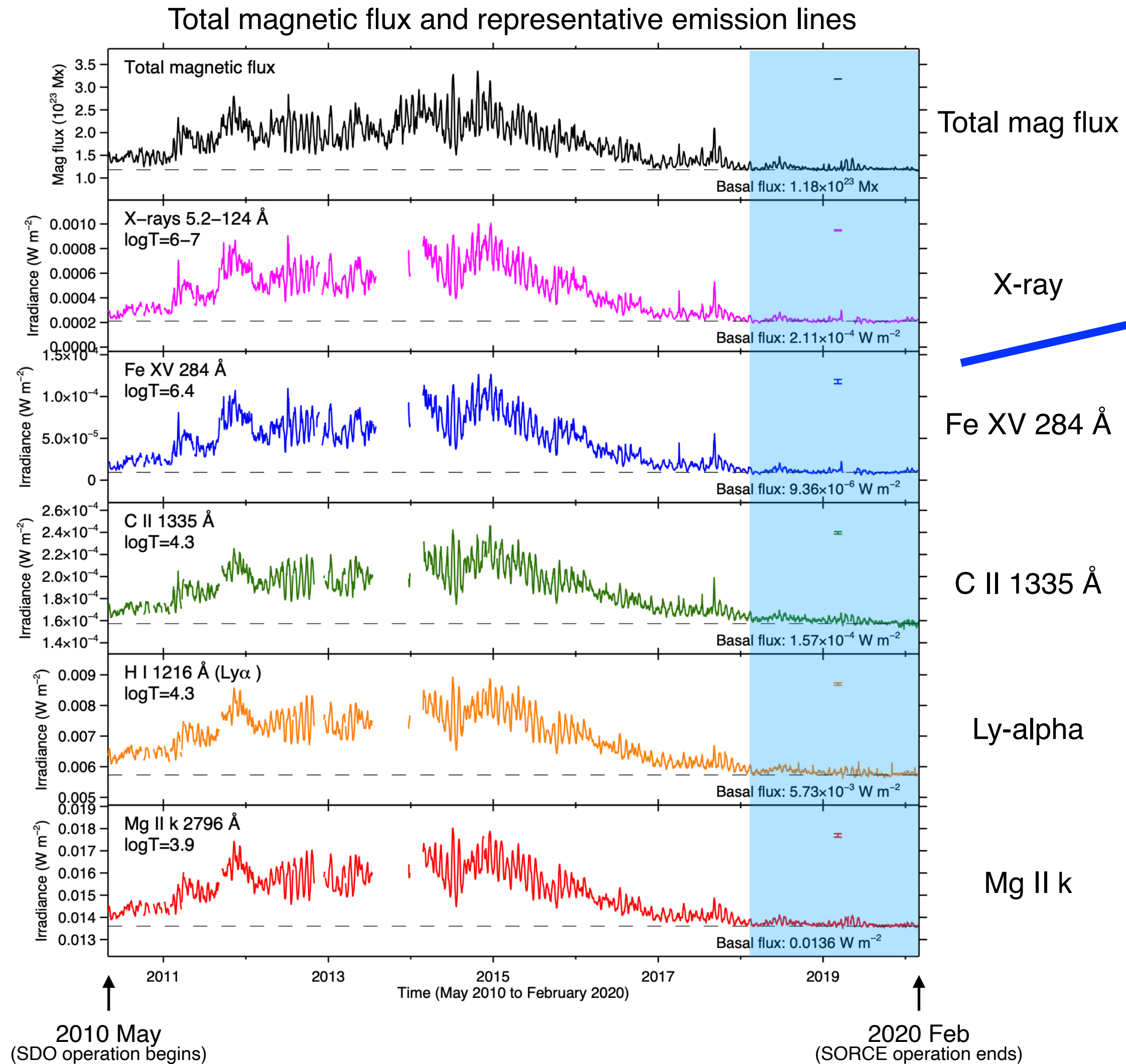
- Analysis of Sun-as-a-star synoptic data over 10 yr
- X-ray, EUV, UV, optical, and radio
- corresponding to corona ($\log T = 6-7$) to chromosphere ($\log T = 4$)
- Compare scaling with stellar data

[1: Fisher+ 1998; Pevtsov+ 2003; Vidotto+ 2014; Reiners+ 2022]

[2: Skumanich 1975; Schrijver+ 1989; Rutten+ 1991; Loukitcheva+ 2009; Barczynski+ 2018]

3. Universality of Atmospheric Heating

- Solar synoptic data over 10 yr



- Calculate basal flux and residual

- Basal fluxes are defined as medians of data from Mar 2019 to Feb 2020 with following criteria
 - ▶ Sunspot number = 0
 - ▶ Total sunspot area = 0
 - ▶ Magnetic flux < 5th percentile of all time

$$\text{Residual} = \text{Light curve} - \text{Basal flux}$$

- ▶ Basal flux: background heating
- ▶ Residual: heating due to magnetic elements

Total radial unsigned magnetic flux

- ▶ daily value
- ▶ generated from four full-disk line-of-sight magnetograms per day

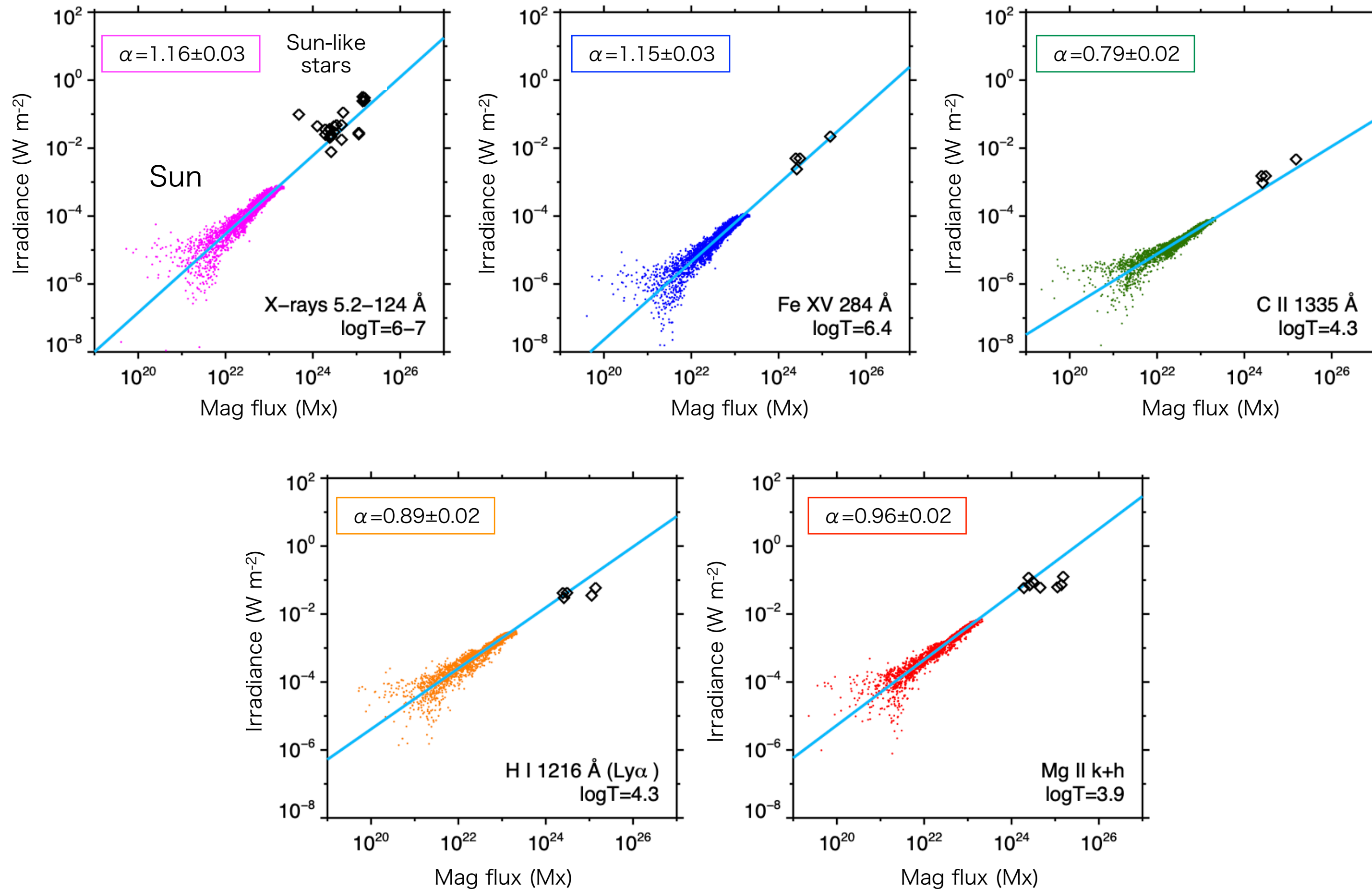
16 spectral lines/bands

- ▶ daily value
- ▶ X-ray to radio
- ▶ $\log T = 3.8 - 7$

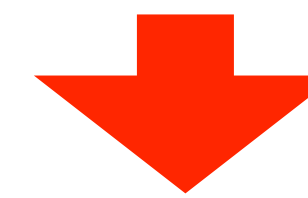
Line centers and widths adopted from Ayres (2021)

3. Universality of Atmospheric Heating

Mag flux—multi-line proportionality $F \propto \Phi^\alpha$



- **Solar data**
 - X-rays show $\alpha=1.16$, consistent with Yokkoh results
 - Other lines also show power-law scalings, although the α values are smaller for cooler temperatures
- **Stellar data**
 - Mainly G-dwarfs with ages from 50 Myr to 4.5 Gyr
 - Total magnetic flux based on Kochukhov et al. (2020)
 - Irradiance from published data
- **Comparison of Sun and stars**
 - Stellar data points are located at extensions of solar scaling laws for all spectral lines (= all temperatures)



✓ Heating mechanism is universal among the Sun and stars, regardless of age or activity

3. Universality of Atmospheric Heating

Irradiance (W m^{-2})

Table 3
Characteristics of the Sun-like Stars

HD	Name	Sp. Type	T_{eff} (K)	$\log g$	Age (Myr)	P_{rot} (days)	R (R_{\odot})	Φ (Mx)	X-rays 5.2–124 Å (W m^{-2})	Fe XV 284 Å (W m^{-2})	C II 1335 Å (W m^{-2})	Ly α (W m^{-2})	Mg II k+h (W m^{-2})
(1)	(2)	(3)	(4)	(5)	(6)	(7)	(8)	(9)	(10)	(11)	(12)	(13)	(14)
1835	BE Cet	G3V	5837	4.47	600	7.78	1.00	4.55×10^{24}	$4.80 \times 10^{-2}, 1.78 \times 10^{-2}$	6.04×10^{-2}
20630	κ^1 Cet	G5V	5742	4.49	600	9.3	0.95	2.61×10^{24}	$2.19 \times 10^{-2}, 2.56 \times 10^{-2}$	2.40×10^{-3}	9.50×10^{-4}	3.01×10^{-2}	7.09×10^{-2}
39587	χ^1 Ori	G0V	5882	4.34	500	4.83	1.05	2.47×10^{24}	$3.48 \times 10^{-2}, 3.73 \times 10^{-2}$	5.00×10^{-3}	1.52×10^{-3}	4.16×10^{-2}	1.18×10^{-1}
56124		G0V	5848	4.46	4500	18	1.01	4.78×10^{23}	9.79×10^{-2}
72905	π^1 Uma	G1.5V	5873	4.44	500	4.9	0.95	3.08×10^{24}	$4.48 \times 10^{-2}, 2.96 \times 10^{-2}$	5.00×10^{-3}	1.52×10^{-3}	4.22×10^{-2}	8.93×10^{-2}
73350	V401 Hya	G5V	5802	4.48	510	12.3	0.98	2.43×10^{24}	2.05×10^{-2}
76151		G3V	5790	4.55	3600	20.5	1.00	2.62×10^{24}	7.78×10^{-3}
82558	LQ Hya	K1V	5000	4.00	50	1.601	0.71	1.39×10^{25}	$3.24 \times 10^{-1}, 2.43 \times 10^{-1}$	5.91×10^{-2}	7.27×10^{-2}
129333	EK Dra	G1.5V	5845	4.47	120	2.606	0.97	1.52×10^{25}	$3.03 \times 10^{-1}, 2.52 \times 10^{-1}$	2.20×10^{-2}	4.70×10^{-3}	...	1.26×10^{-1}
131156	ξ Boo A	G7V	5570	4.65	200	6.4	0.83	1.13×10^{25}	$2.58 \times 10^{-2}, 2.83 \times 10^{-2}$	3.53×10^{-2}	6.19×10^{-2}
166435		G1IV	5843	4.44	3800	3.43	0.99	4.94×10^{24}	1.12×10^{-1}
175726		G0V	5998	4.41	500	3.92	1.06	1.26×10^{24}	4.48×10^{-2}
190771		G2V	5834	4.44	2700	8.8	1.01	3.48×10^{24}	4.80×10^{-2}
206860	HN Peg	G0V	5974	4.47	260	4.55	1.04	1.92×10^{24}	$3.56 \times 10^{-2}, 2.52 \times 10^{-2}$	5.90×10^{-2}
Sun	(mean)	G2V	5777	4.44	4600	25.4	1.00	1.73×10^{23}	4.24×10^{-4}	4.12×10^{-5}	1.84×10^{-4}	6.77×10^{-3}	2.55×10^{-2}
	(median)							1.67×10^{23}	3.87×10^{-4}	3.59×10^{-5}	1.82×10^{-4}	6.69×10^{-3}	2.52×10^{-2}
	(max)							3.35×10^{23}	1.01×10^{-3}	1.27×10^{-4}	2.46×10^{-4}	8.94×10^{-3}	3.06×10^{-2}
	(min)							1.16×10^{23}	1.85×10^{-4}	5.68×10^{-6}	1.52×10^{-4}	5.60×10^{-3}	2.32×10^{-2}

Note. The HD number, name, spectral type, effective temperature, surface gravity, age, rotation period, and radius of the stars are shown in Columns 1–8. Column 9 shows the total hemispheric magnetic flux estimated based on the Zeeman broadening of the spectral lines. Columns 10–14 show the irradiances of X-ray 5.2–124 Å, Fe XV 284 Å, C II 1334.5 + 1335.7 Å, Ly α , and Mg II k+h (combined) in the literature, all converted to the values at 1 au from the stars. For X-rays, multiple observations are shown (if they exist).

References. Turon et al. (1993), Valenti & Fischer (2005), McDonald et al. (2012), Gonzalez et al. (2010), Cole et al. (2015), Allende Prieto & Lambert (1999), Vidotto et al. (2014), Rosén et al. (2016), Oláh et al. (2016), See et al. (2019), Kochukhov et al. (2020), Telleschi et al. (2005), Ribas et al. (2005), Takeda et al. (2007), Wood & Linsky (2010), Güdel et al. (1997), Wood et al. (2005), Schmitt et al. (1990), Dorren & Guinan (1994).

ults
ugh

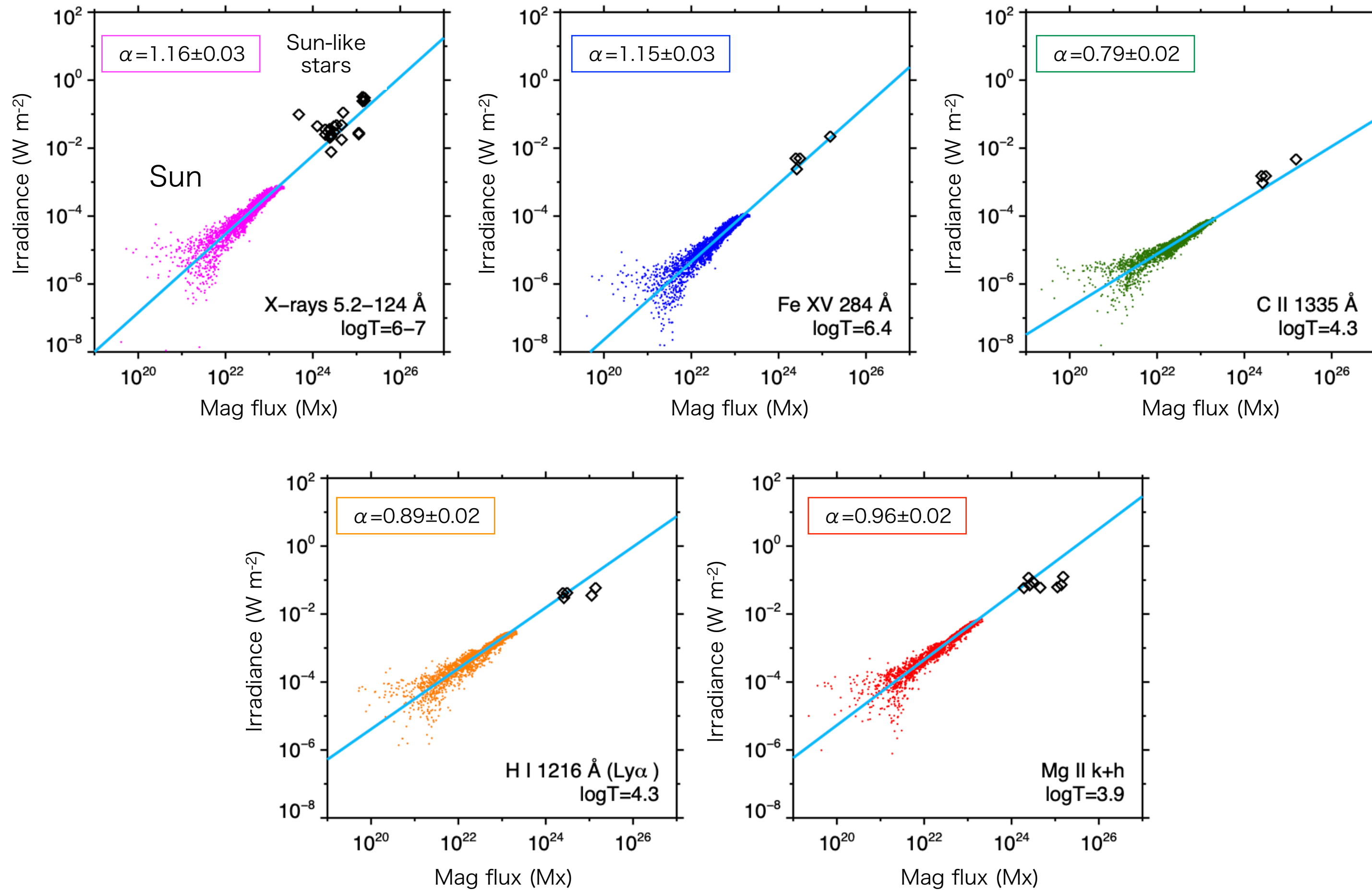
yr
2020)

solar
ures)

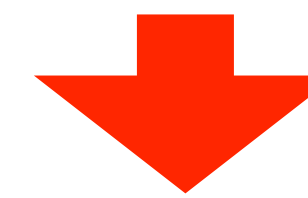
the
ivity

3. Universality of Atmospheric Heating

Mag flux—multi-line proportionality $F \propto \Phi^\alpha$

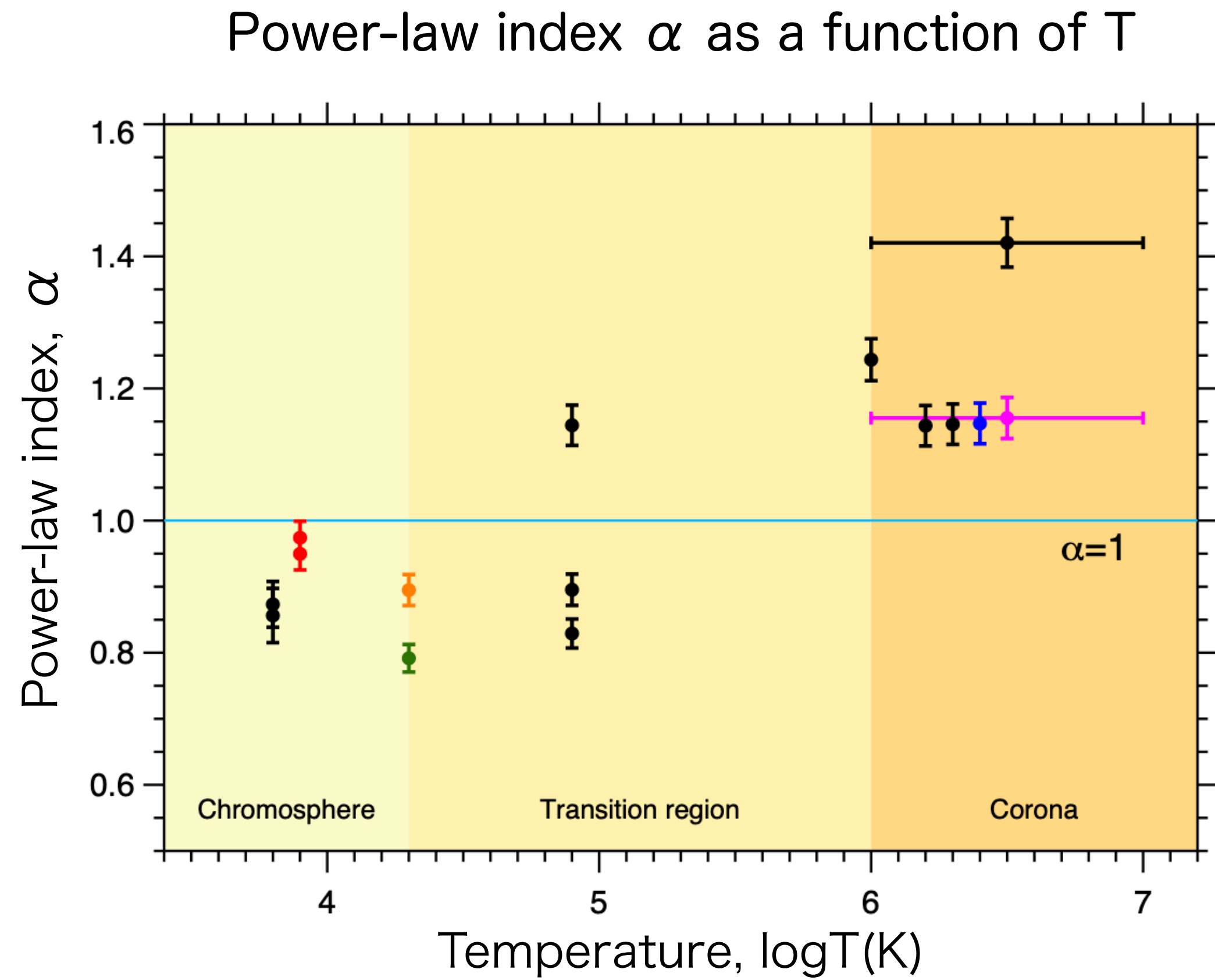


- **Solar data**
 - X-rays show $\alpha=1.16$, consistent with Yokkoh results
 - Other lines also show power-law scalings, although the α values are smaller for cooler temperatures
- **Stellar data**
 - Mainly G-dwarfs with ages from 50 Myr to 4.5 Gyr
 - Total magnetic flux based on Kochukhov et al. (2020)
 - Irradiance from published data
- **Comparison of Sun and stars**
 - Stellar data points are located at extensions of solar scaling laws for all spectral lines (= all temperatures)

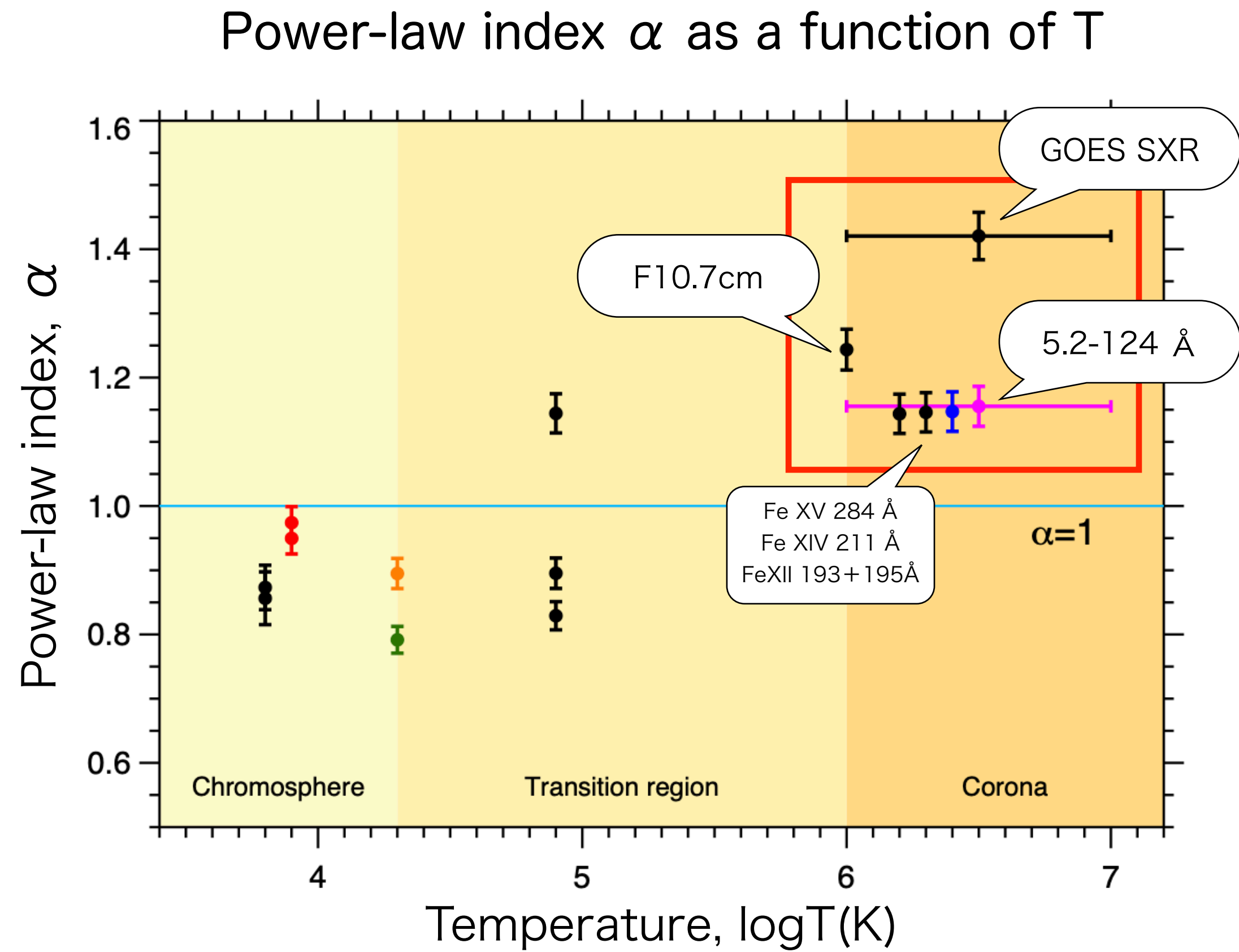


✓ Heating mechanism is universal among the Sun and stars, regardless of age or activity

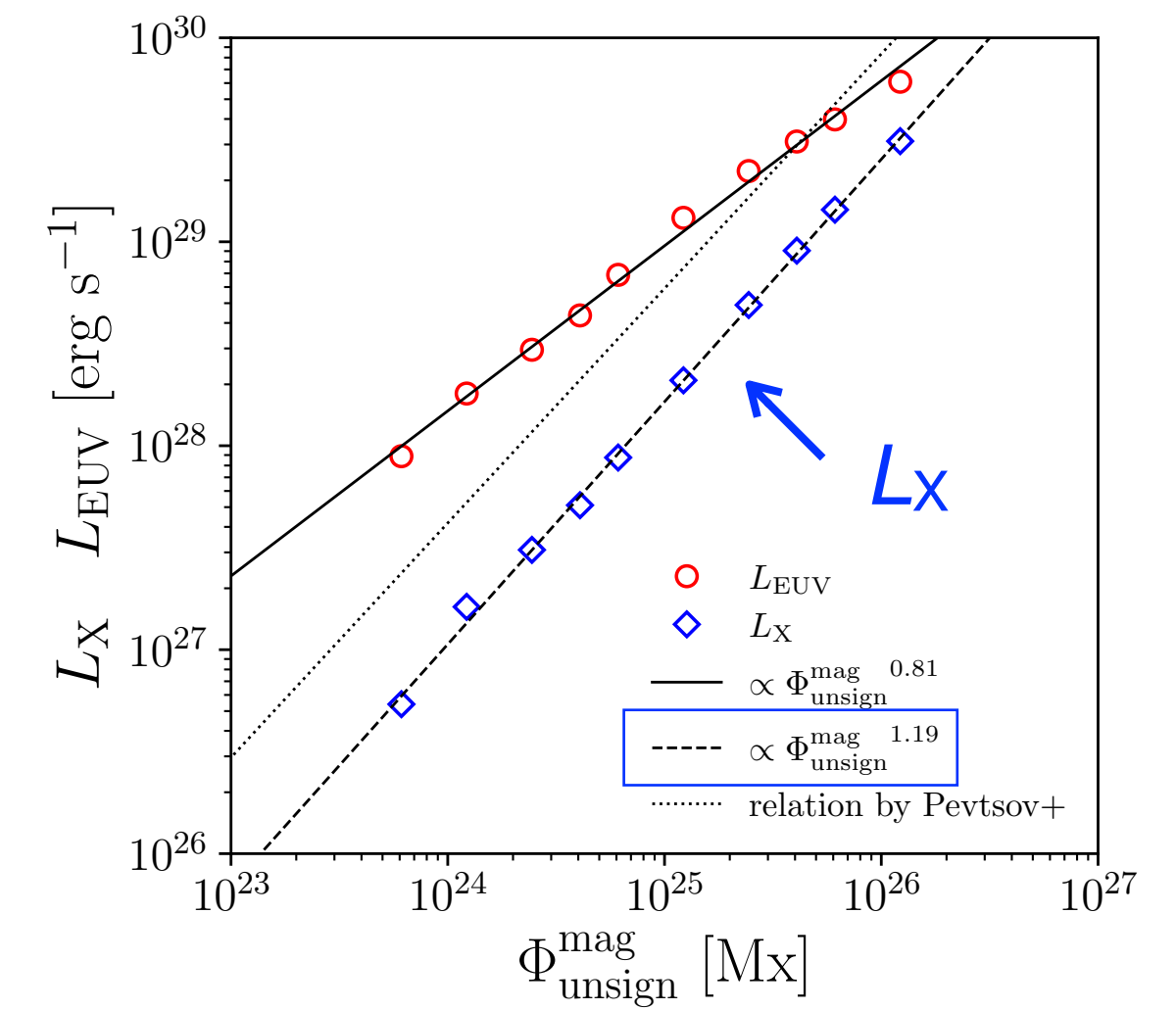
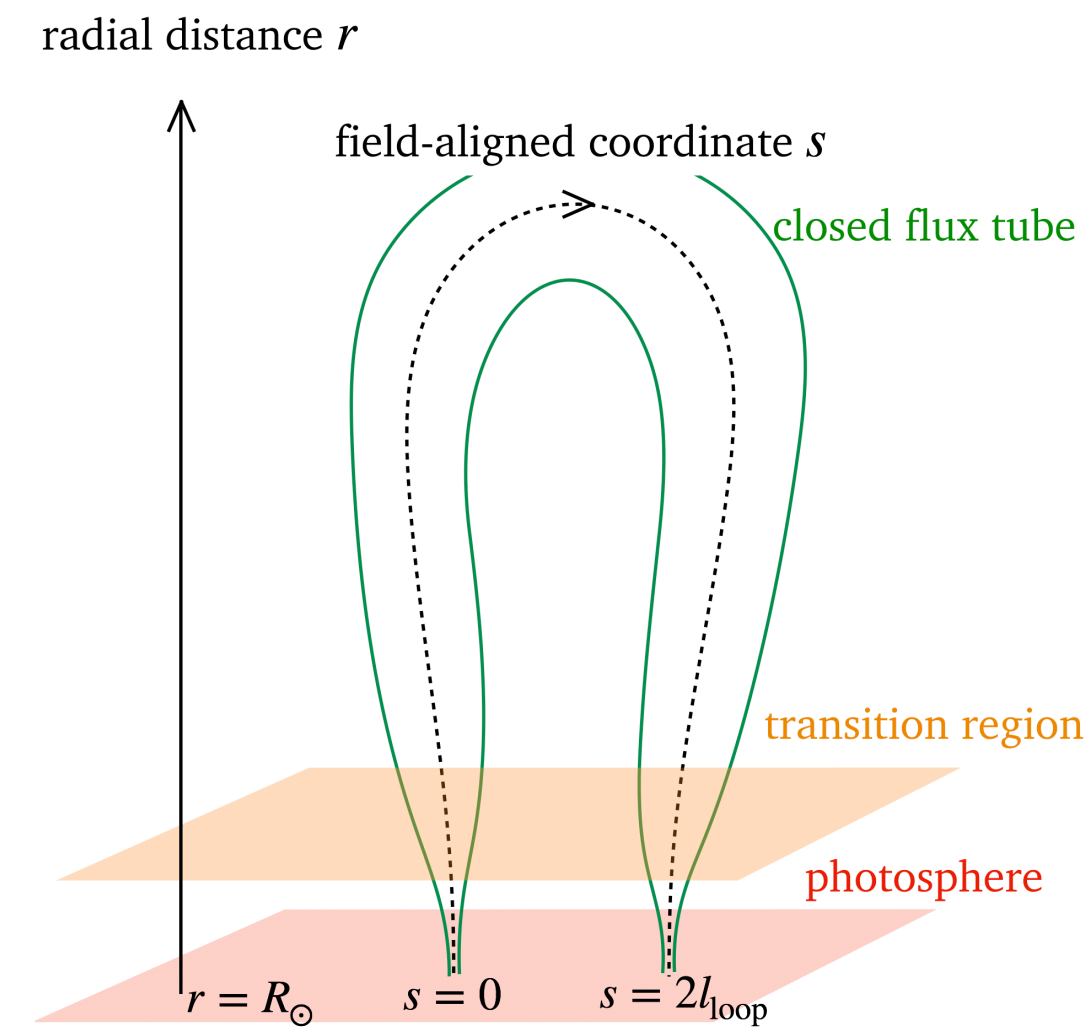
3. Universality of Atmospheric Heating



3. Universality of Atmospheric Heating

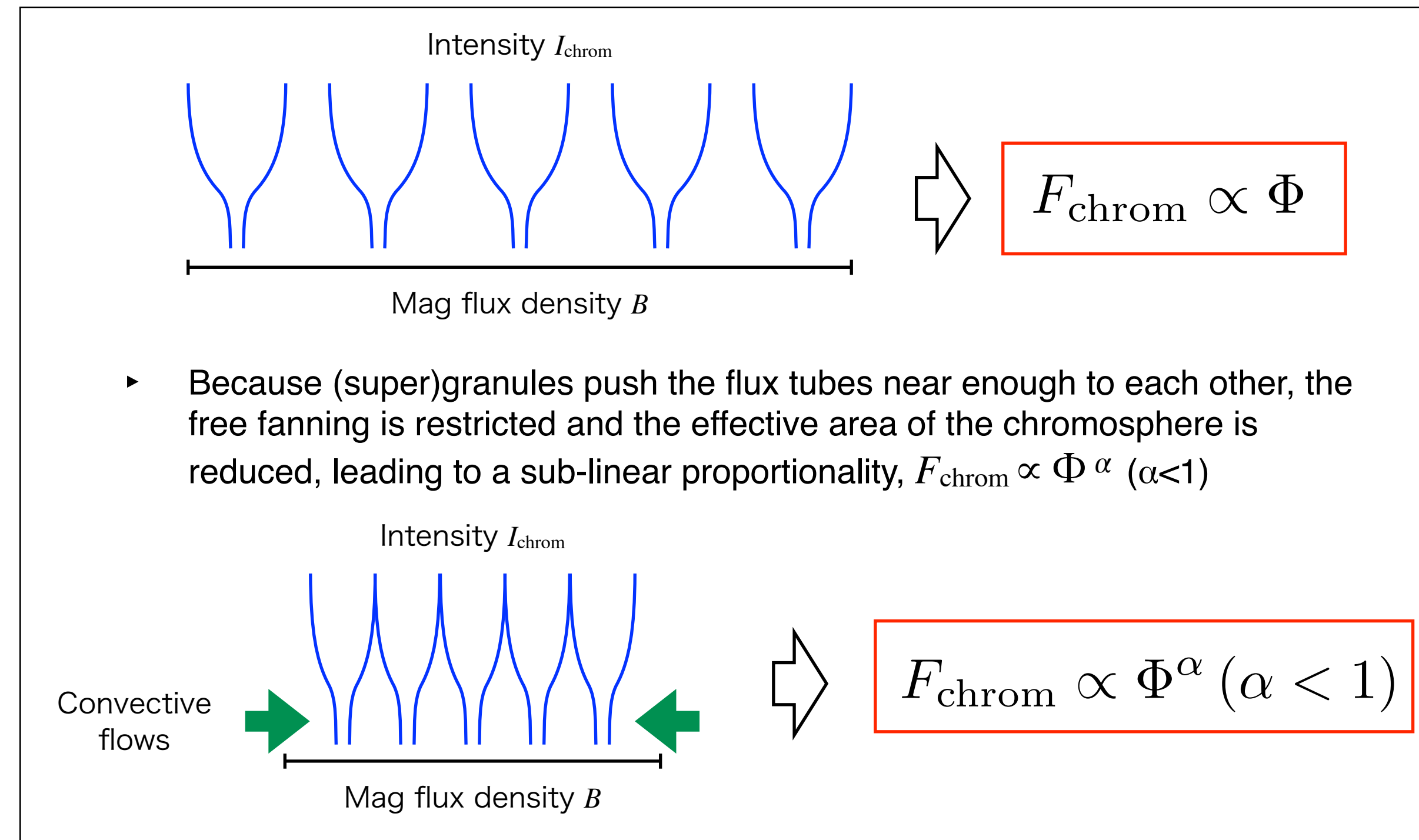
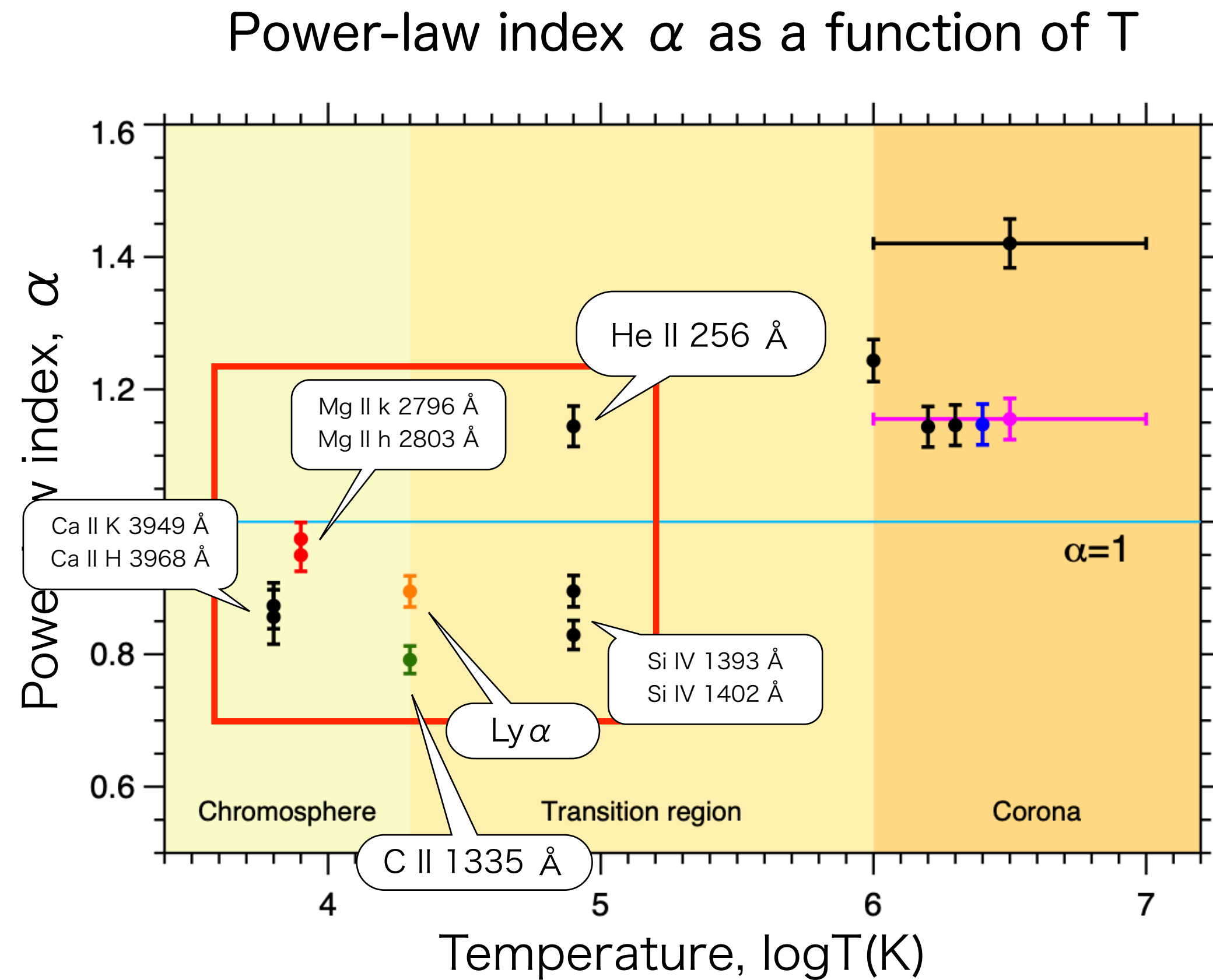


- Corona: $\log T > 6$
 - Not only X-rays but also **other coronal proxies consistently show $\alpha > 1$**
 - Explained by theoretical and numerical models [Zhuleku et al. 2020; also Fisher+1998; Takasao+ 2020]



3. Universality of Atmospheric Heating

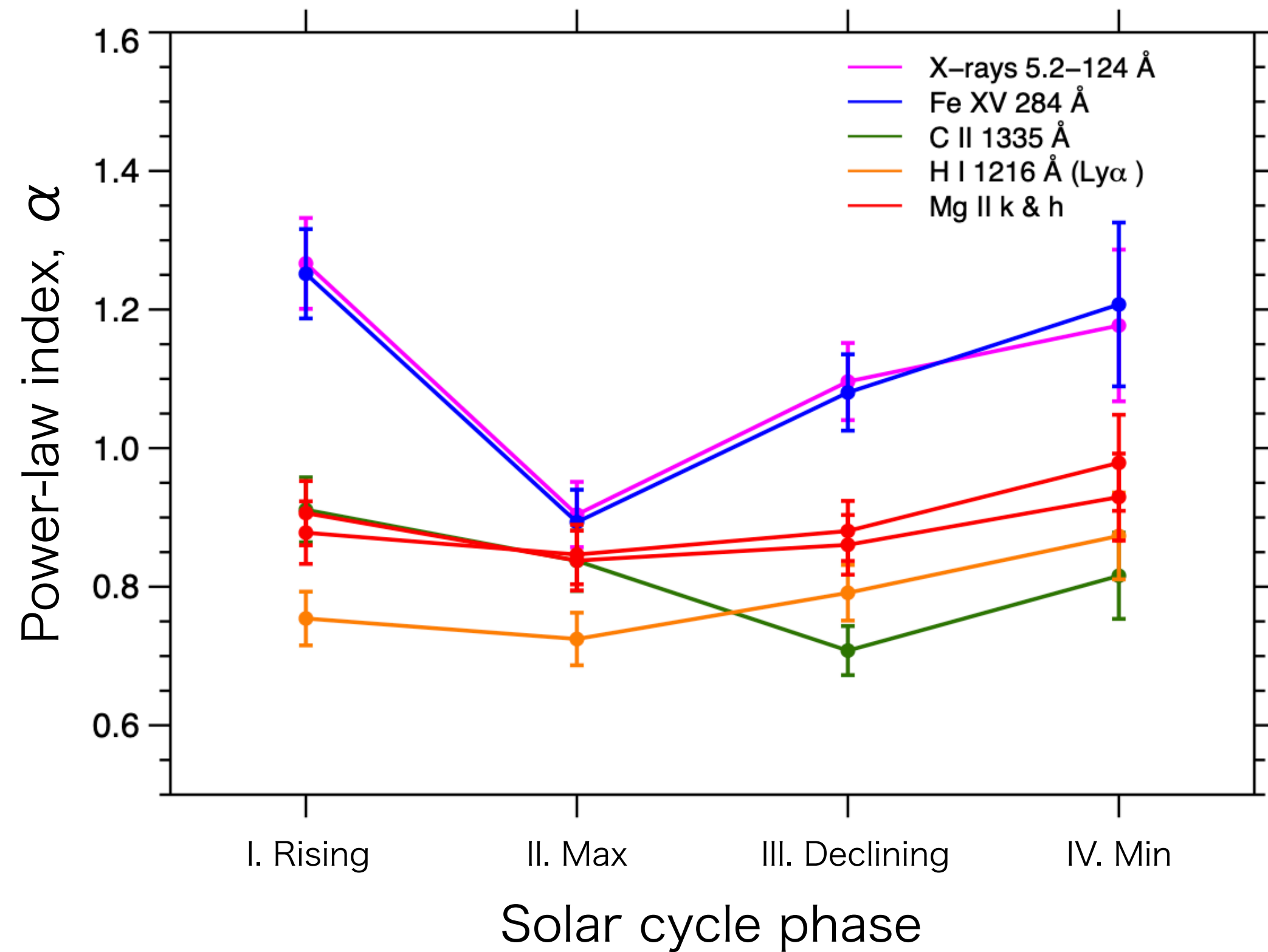
- TR to chromosphere: $\log T < 6$
 - **Power-law exponents fall below unity, $\alpha < 1$** , indicating that the efficiency of chromospheric heating is weaker than the corona
 - In line with the previous studies [Skumanich et al. 1975; Schrijver et al. 1989; Loukitcheva et al. 2009; Barczynski et al. 2018]
 - Geometrical model by Schrijver et al. (1989) :



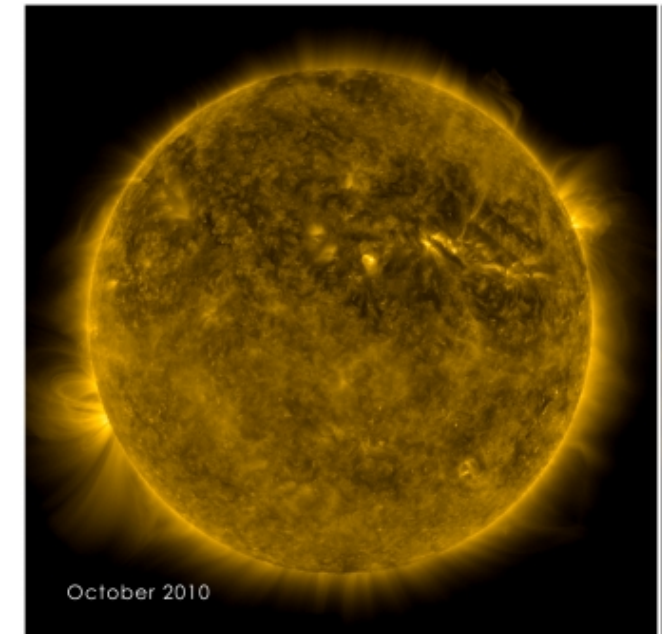
- Flux tube expansion is also a key for Alfvén wave reflection [Cranmer & van Ballegoijen 2005]
- May require **numerical modeling** to understand why $\alpha < 1$

3. Universality of Atmospheric Heating

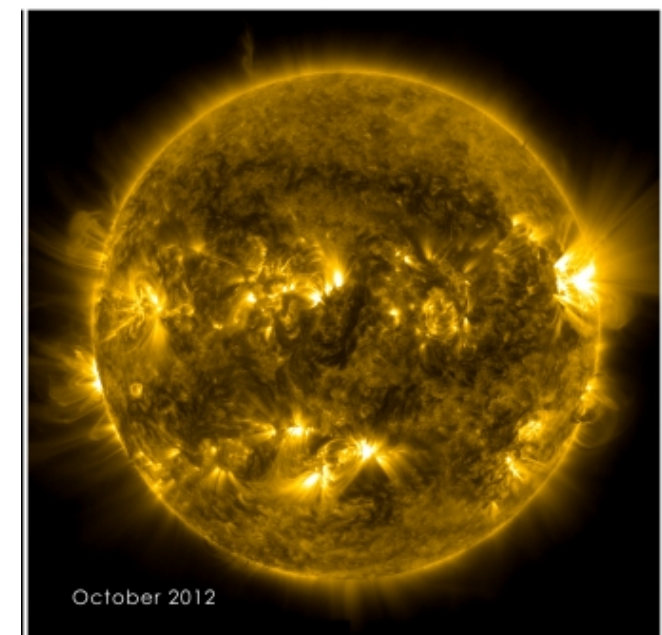
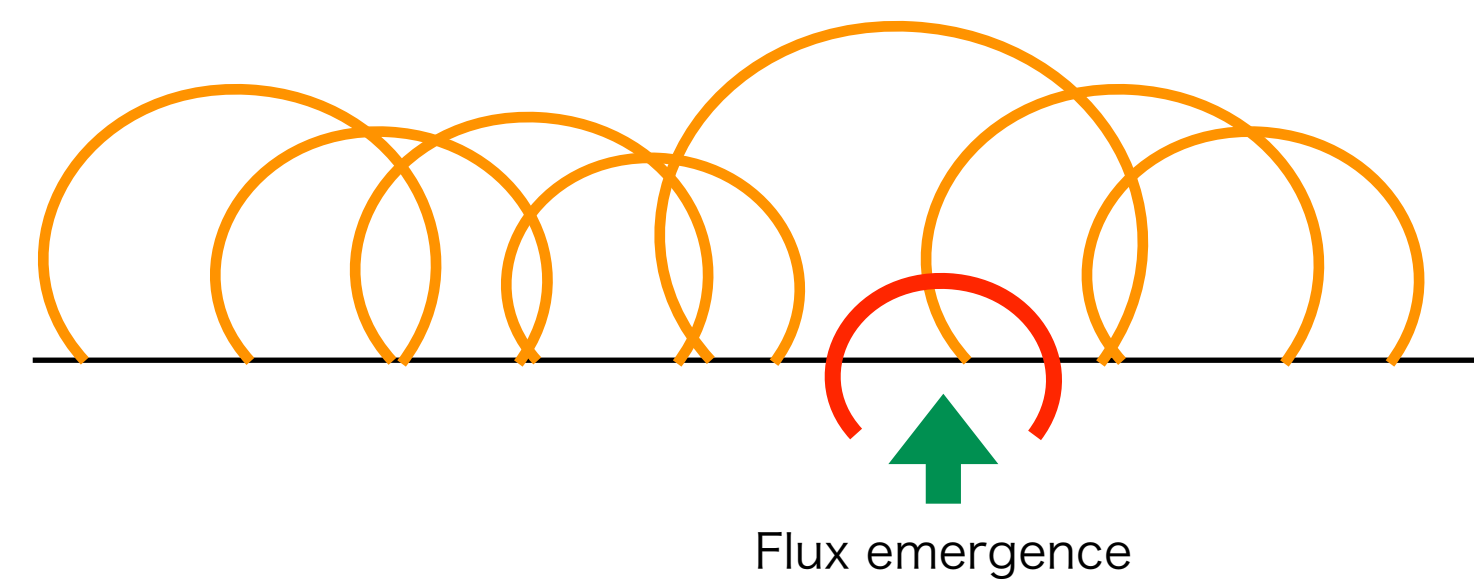
Solar cycle dependence of α



- α is smallest at solar maximum
 - At minimum, the Sun has few active regions.

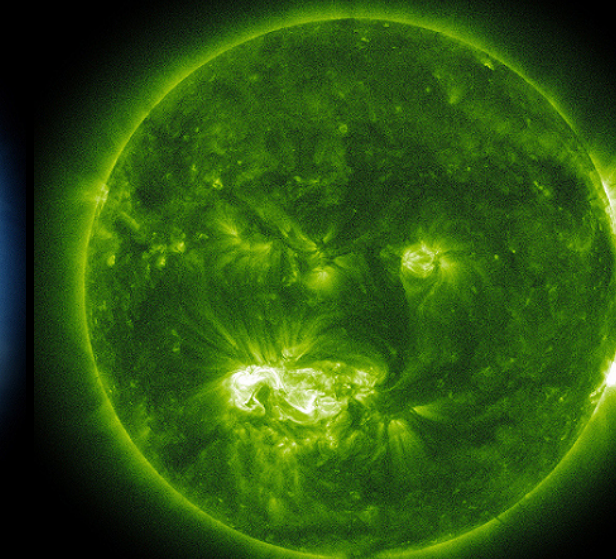
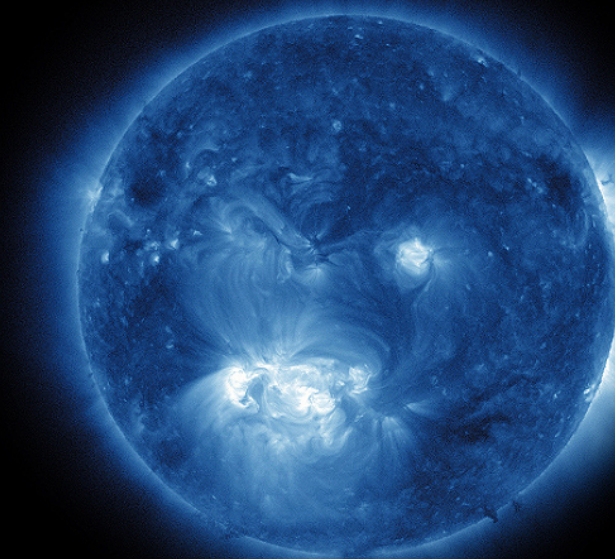
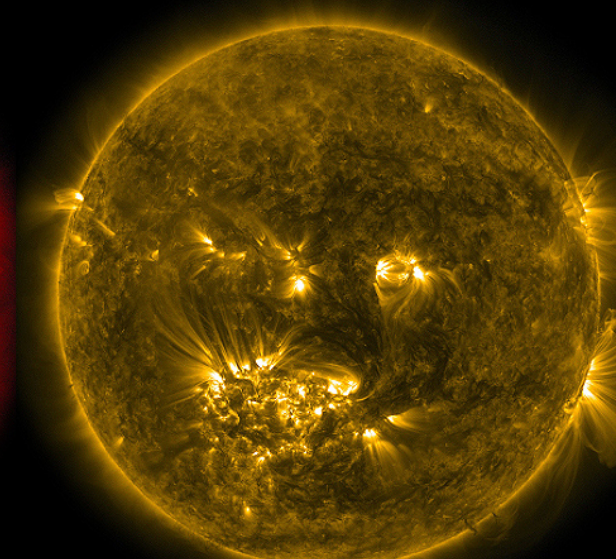
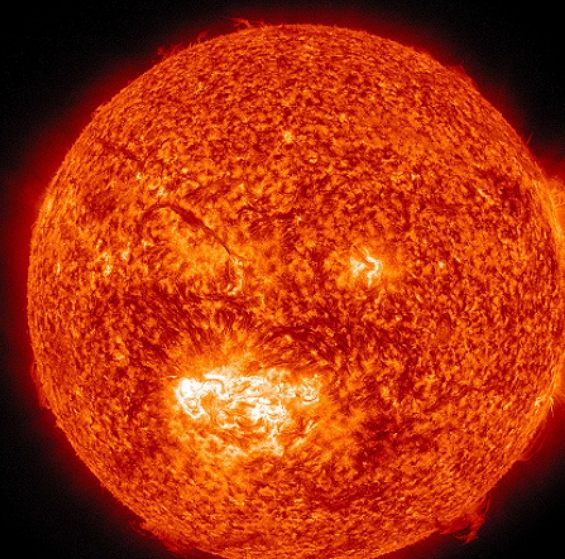
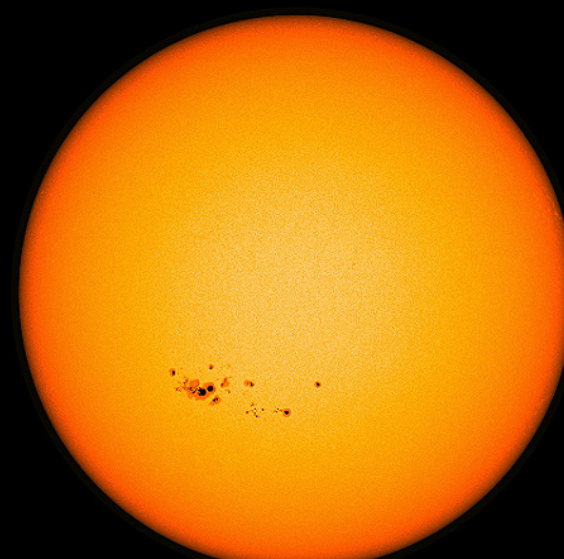
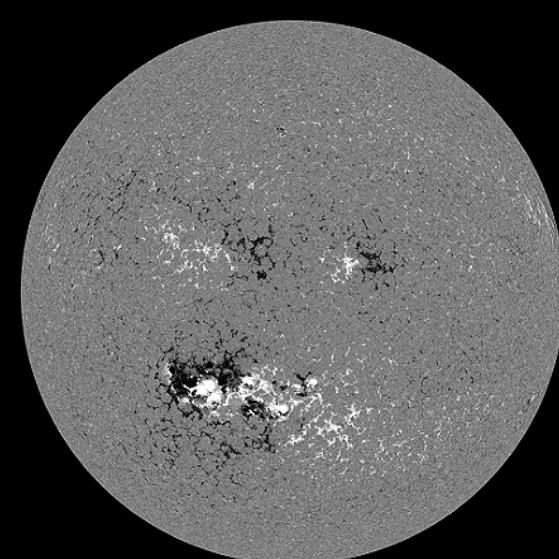


- At maximum, the Sun is filled with magnetic fluxes and loops. Therefore, the atmosphere is not effectively heated any more even if the new mag flux is supplied to the surface via flux emergence.



- Requires global effect in numerical modeling?

3. Universality of Atmospheric Heating: Catalog Updated



Activity proxy

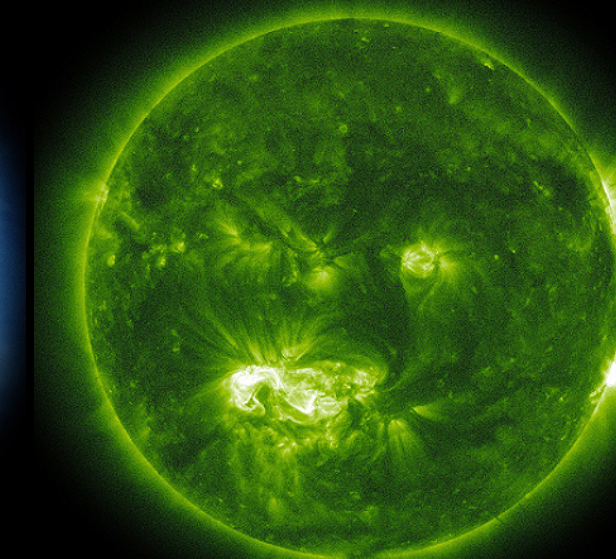
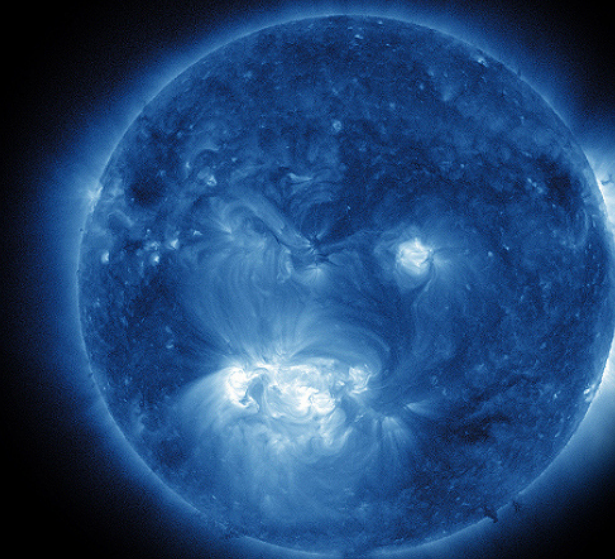
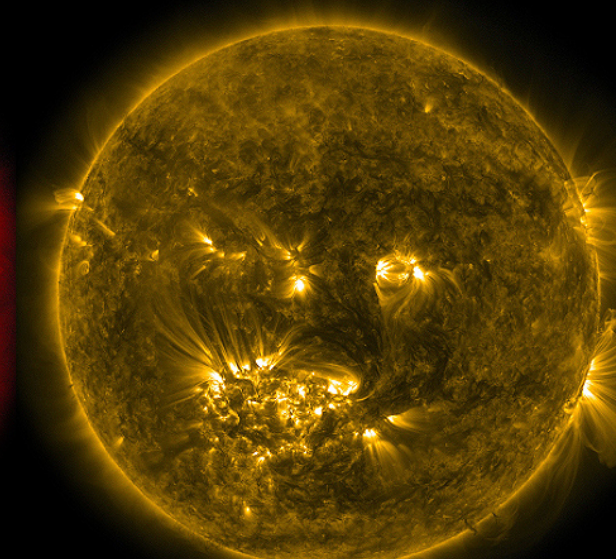
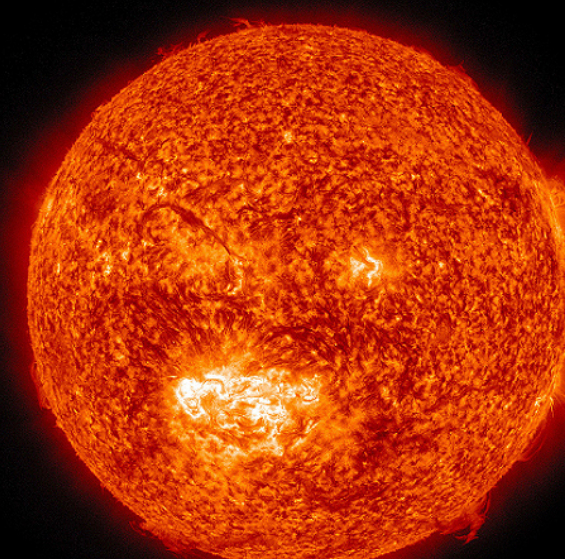
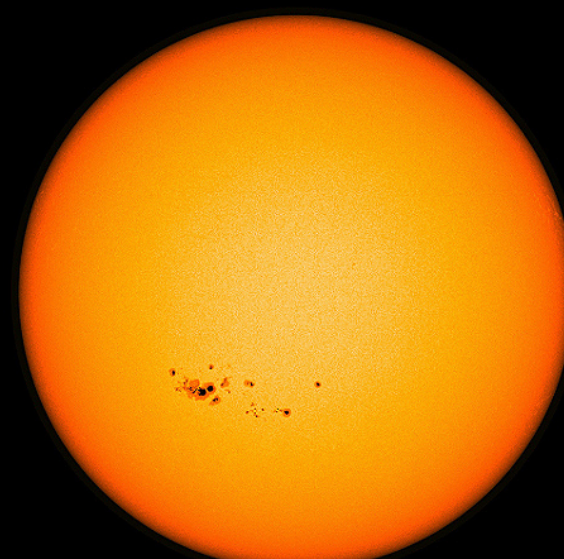
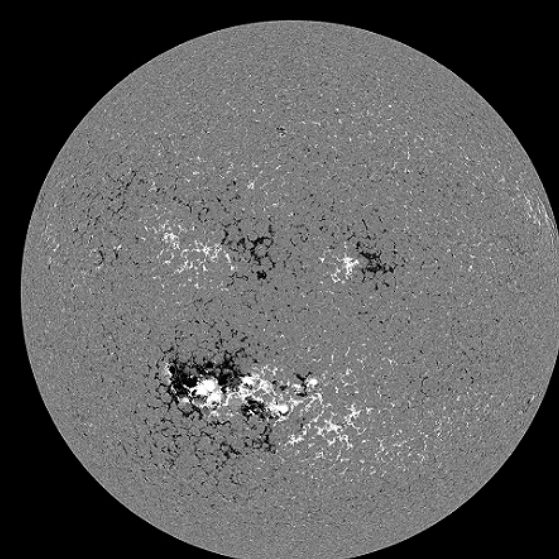
Irradiance ($3.8 < \log T < 7$)

- Radial magnetic flux

**Catalog of
power-law index**

- X-rays 1–8 Å
- X-rays 5.2–124 Å
- Fe XV 284 Å
- Fe XIV 211 Å
- Fe XII 193+195 Å
- F10.7 cm radio
- He II 256 Å + blends
- Si IV 1393 Å
- Si IV 1402 Å
- C II 1335 Å
- H I 1216 Å (Ly α)
- Mg II k 2796 Å
- Mg II h 2803 Å
- Ca II K 3934 Å
- Ca II H 3968 Å
- H I 6563 Å (H α)

3. Universality of Atmospheric Heating: Catalog Updated



Activity proxy

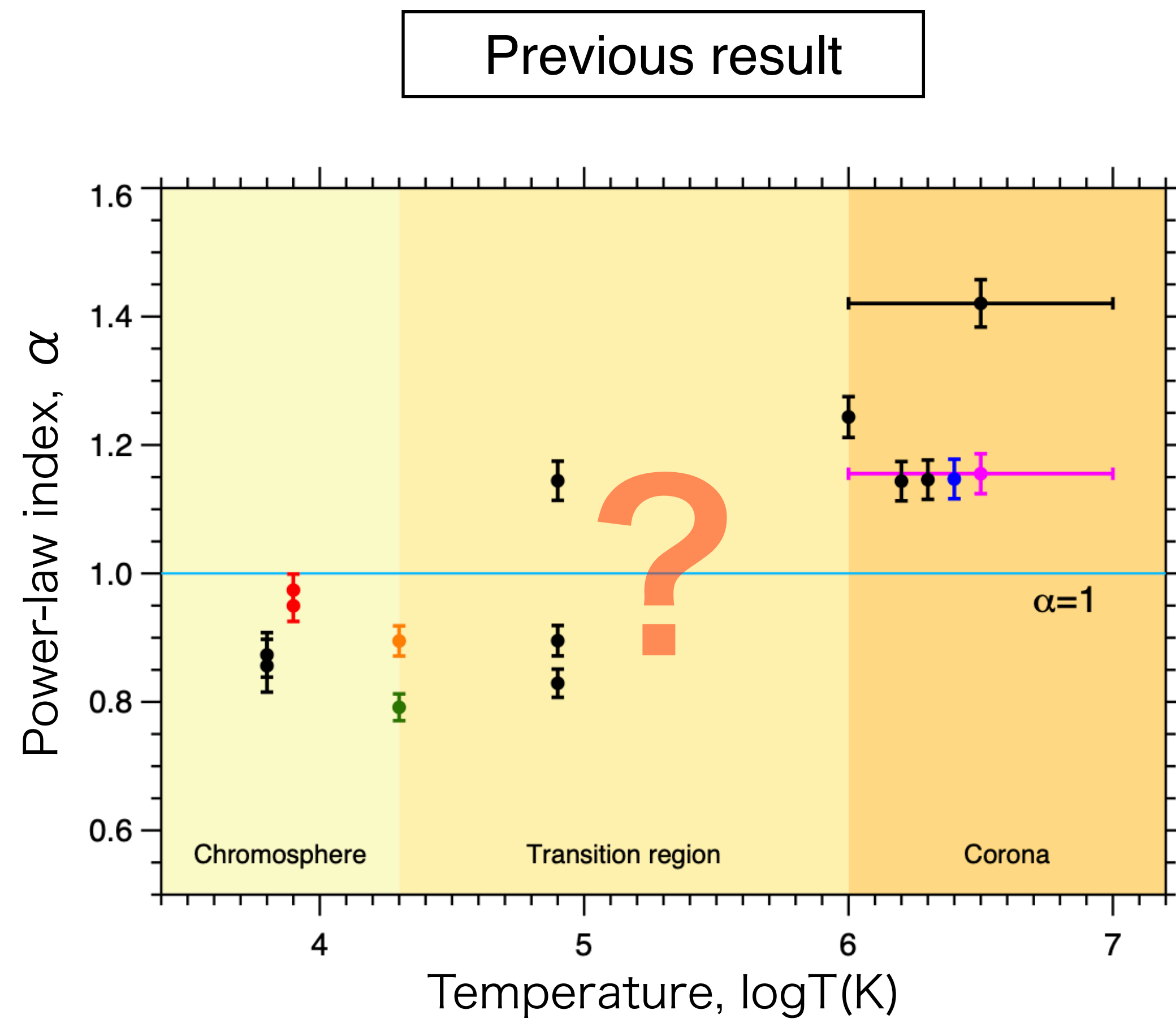
- Radial magnetic flux

Irradiance ($3.8 < \log T < 7$)

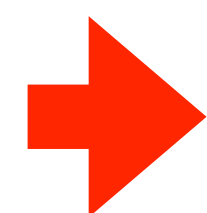
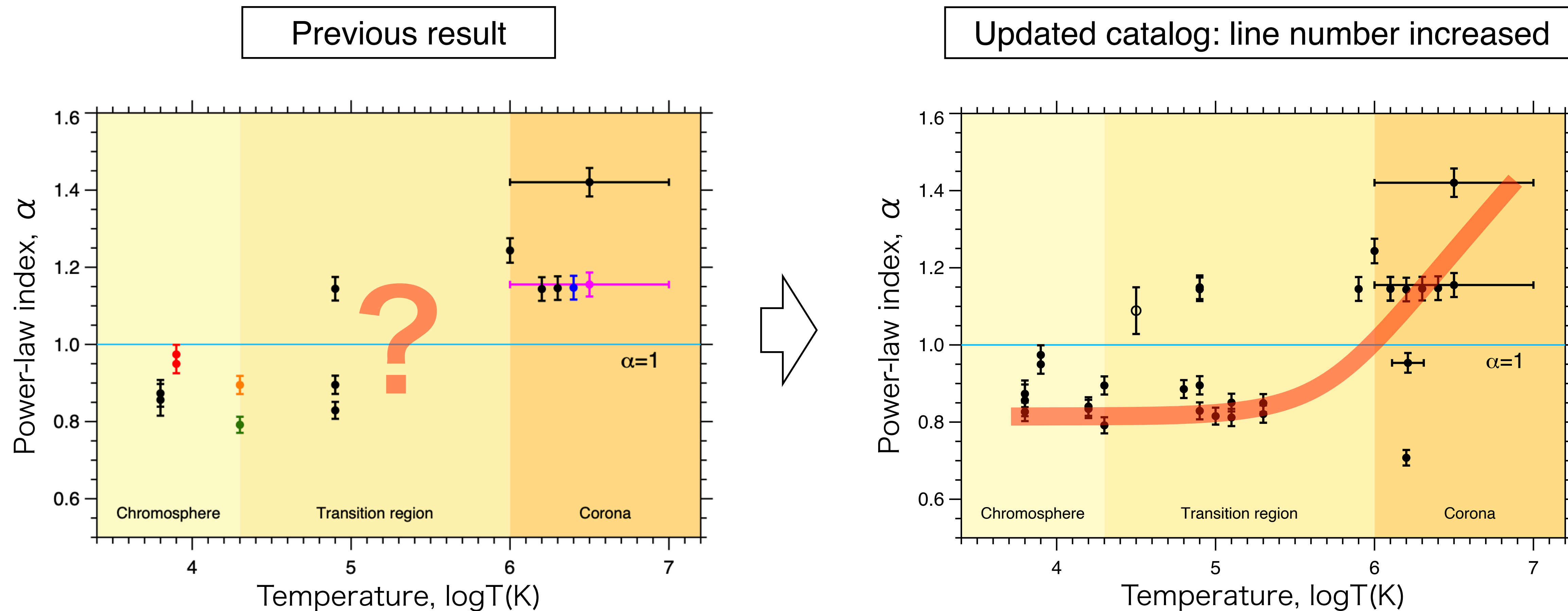
Catalog of power-law index

- | | |
|-----------------------|-----------------------------|
| • X-rays 1–8 Å | • He II 304 Å |
| • X-rays 5.2–124 Å | • Si IV 1393 Å |
| • Fe XV 284 Å | • Si IV 1402 Å |
| • Fe XIV 211 Å | • Si III 1206 Å |
| • X-rays (XRT) | • He I 10830 Å |
| • Fe XII 193+195 Å | • C II 1335 Å |
| • Fe XII 1349 Å | • H I 1216 Å (Ly α) |
| • Fe X 174 Å | • O I 1302 Å |
| • Fe XI 180 Å | • O I 1305 Å |
| • F10.7cm radio | • Mg II k 2796 Å |
| • Fe IX 171 Å | • Mg II h 2803 Å |
| • N V 1238 Å | • C II 1351 Å |
| • N V 1242 Å | • Ca II K 3934 Å |
| • C IV 1548 Å | • Ca II H 3968 Å |
| • C IV 1551 Å | • H I 6563 Å (H α) |
| • C III 1175 Å | • Ca II 8542 Å |
| • He II 256 Å +blends | |

3. Universality of Atmospheric Heating: Catalog Updated

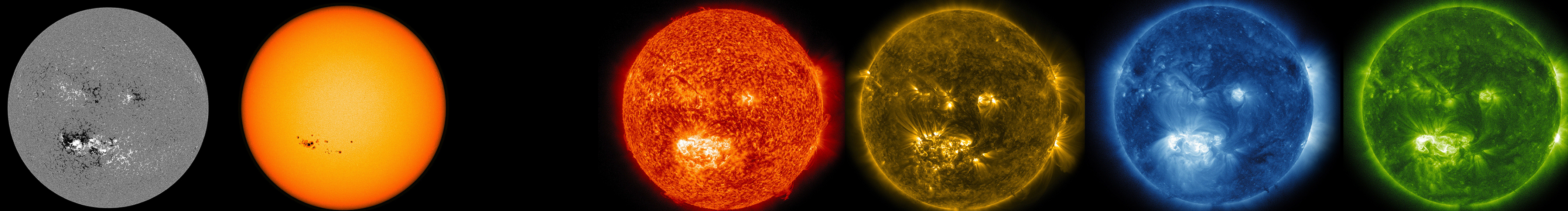


3. Universality of Atmospheric Heating: Catalog Updated



✓ Similarity of heating efficiencies (mechanisms) of transition region and chromosphere

3. Universality of Atmospheric Heating: Catalog Updated



Activity proxy

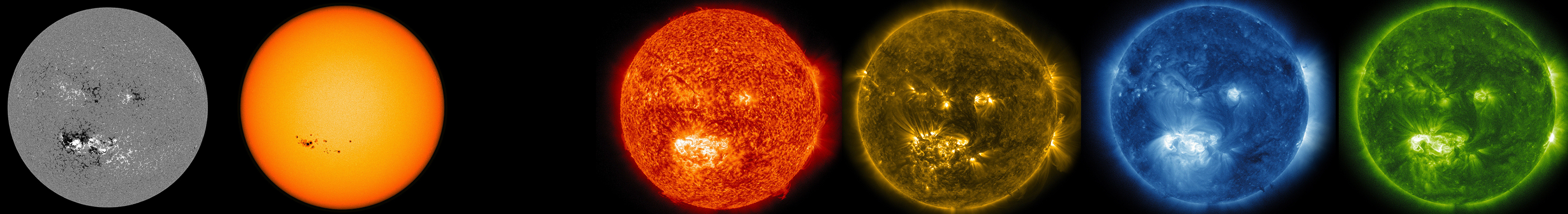
- Radial magnetic flux

Irradiance ($3.8 < \log T < 7$)

**Catalog of
power-law index**

- | | |
|-----------------------|-----------------------------|
| • X-rays 1–8 Å | • He II 304 Å |
| • X-rays 5.2–124 Å | • Si IV 1393 Å |
| • Fe XV 284 Å | • Si IV 1402 Å |
| • Fe XIV 211 Å | • Si III 1206 Å |
| • X-rays (XRT) | • He I 10830 Å |
| • Fe XII 193+195 Å | • C II 1335 Å |
| • Fe XII 1349 Å | • H I 1216 Å (Ly α) |
| • Fe X 174 Å | • O I 1302 Å |
| • Fe XI 180 Å | • O I 1305 Å |
| • F10.7cm radio | • Mg II k 2796 Å |
| • Fe IX 171 Å | • Mg II h 2803 Å |
| • N V 1238 Å | • C II 1351 Å |
| • N V 1242 Å | • Ca II K 3934 Å |
| • C IV 1548 Å | • Ca II H 3968 Å |
| • C IV 1551 Å | • H I 6563 Å (H α) |
| • C III 1175 Å | • Ca II 8542 Å |
| • He II 256 Å +blends | |

3. Universality of Atmospheric Heating: Catalog Updated



Activity proxy

- Radial magnetic flux
- LOS magnetic flux
- Sunspot number
- Sunspot area
- F10.7 cm radio

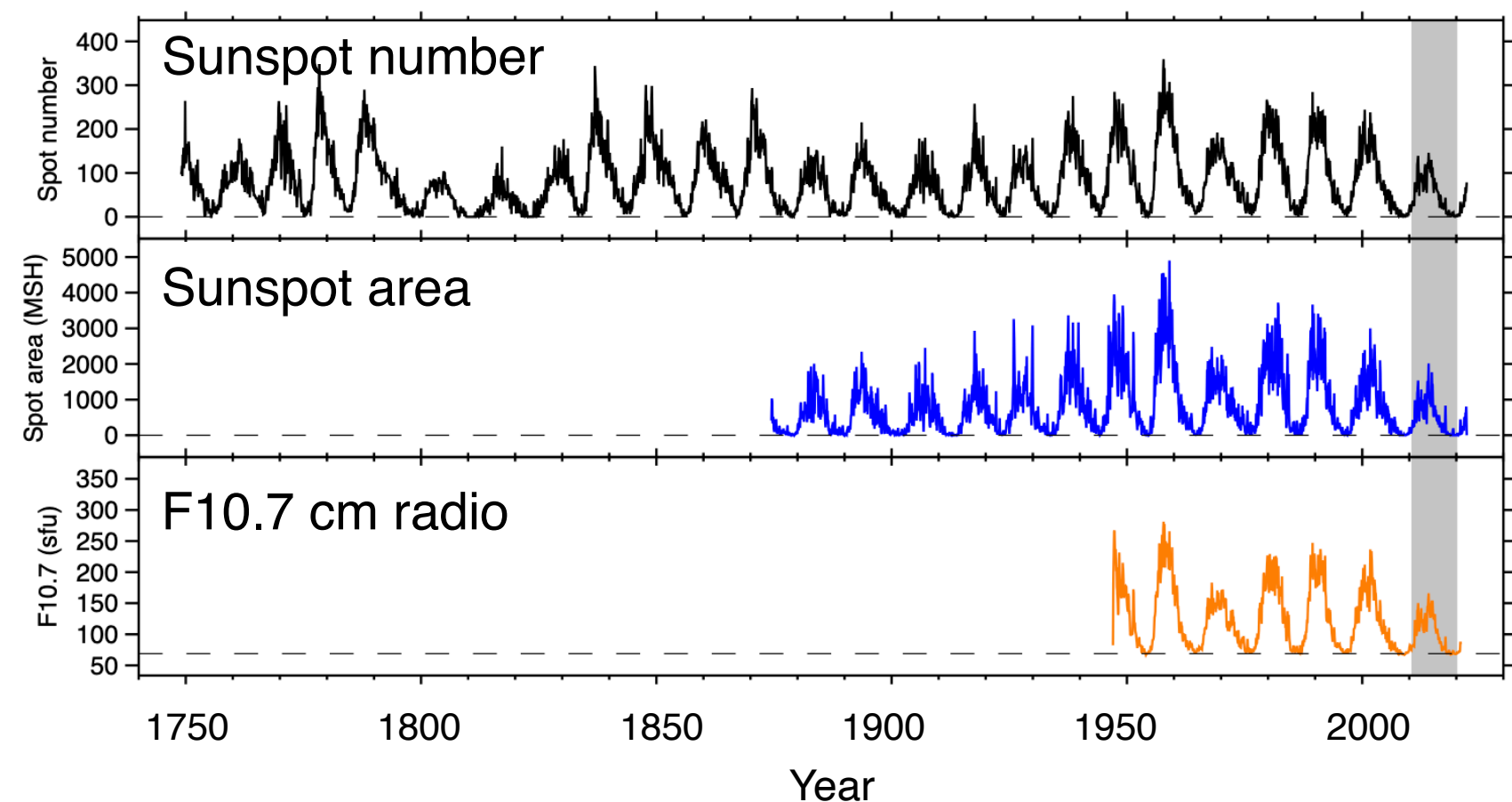
Irradiance ($3.8 < \log T < 7$)

Catalog of power-law index

- | | |
|-----------------------|-----------------------------|
| • X-rays 1–8 Å | • He II 304 Å |
| • X-rays 5.2–124 Å | • Si IV 1393 Å |
| • Fe XV 284 Å | • Si IV 1402 Å |
| • Fe XIV 211 Å | • Si III 1206 Å |
| • X-rays (XRT) | • He I 10830 Å |
| • Fe XII 193+195 Å | • C II 1335 Å |
| • Fe XII 1349 Å | • H I 1216 Å (Ly α) |
| • Fe X 174 Å | • O I 1302 Å |
| • Fe XI 180 Å | • O I 1305 Å |
| • F10.7cm radio | • Mg II k 2796 Å |
| • Fe IX 171 Å | • Mg II h 2803 Å |
| • N V 1238 Å | • C II 1351 Å |
| • N V 1242 Å | • Ca II K 3934 Å |
| • C IV 1548 Å | • Ca II H 3968 Å |
| • C IV 1551 Å | • H I 6563 Å (H α) |
| • C III 1175 Å | • Ca II 8542 Å |
| • He II 256 Å +blends | |

3. Universality of Atmospheric Heating: Catalog Updated

Historical solar observations



Catalog of α

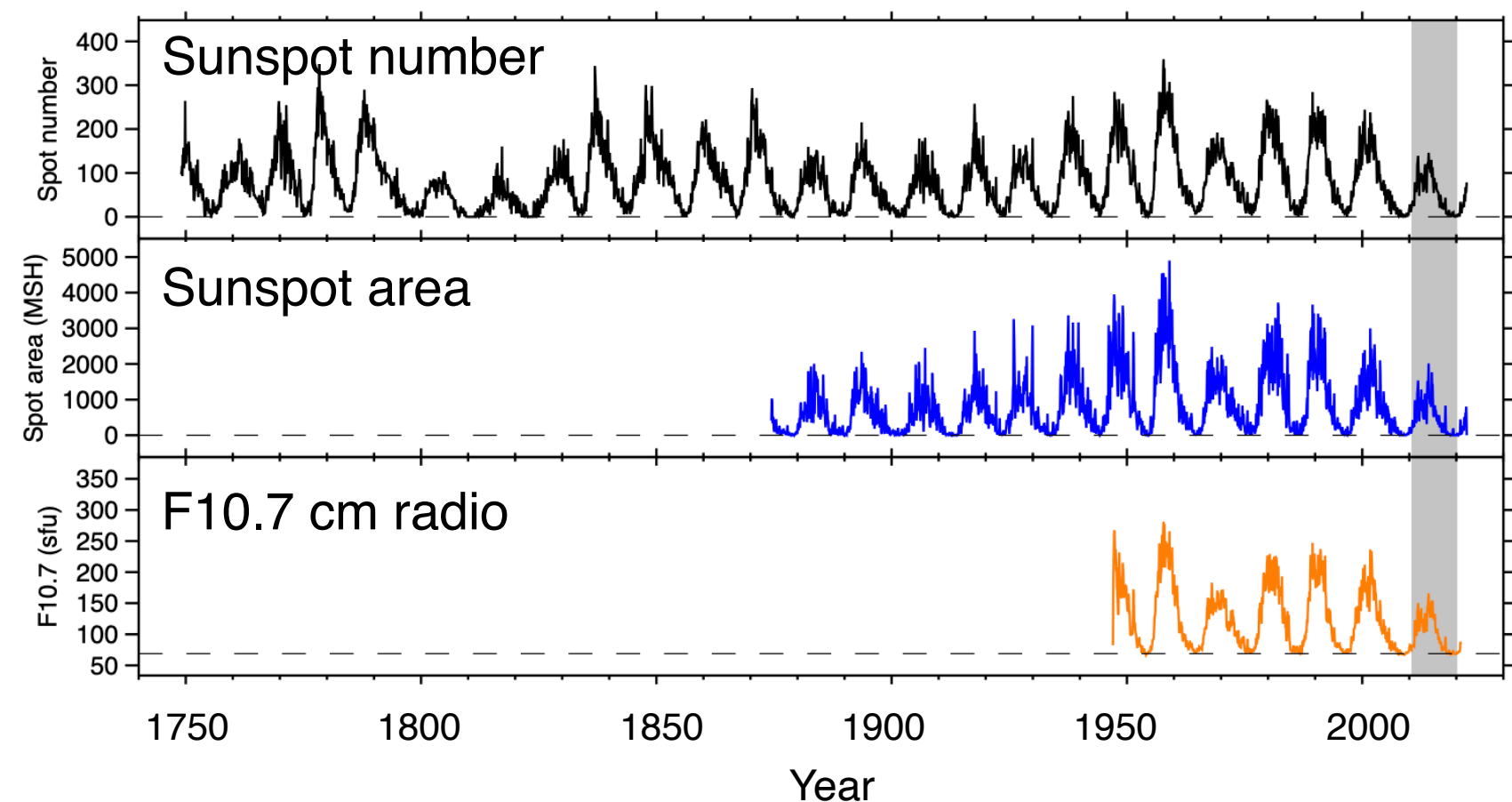
$$F^{\text{line}}(t) = 10^{\beta} [P(t) - P_0]^{\alpha} + F_0^{\text{line}}$$

Irradiances can be reconstructed from

- Historical solar observations
- Stellar observations
- Surface flux transport simulations
- Dynamo models
- etc.

3. Universality of Atmospheric Heating: Catalog Updated

Historical solar observations



Catalog of α

$$F^{\text{line}}(t) = 10^{\beta} [P(t) - P_0]^{\alpha} + F_0^{\text{line}}$$

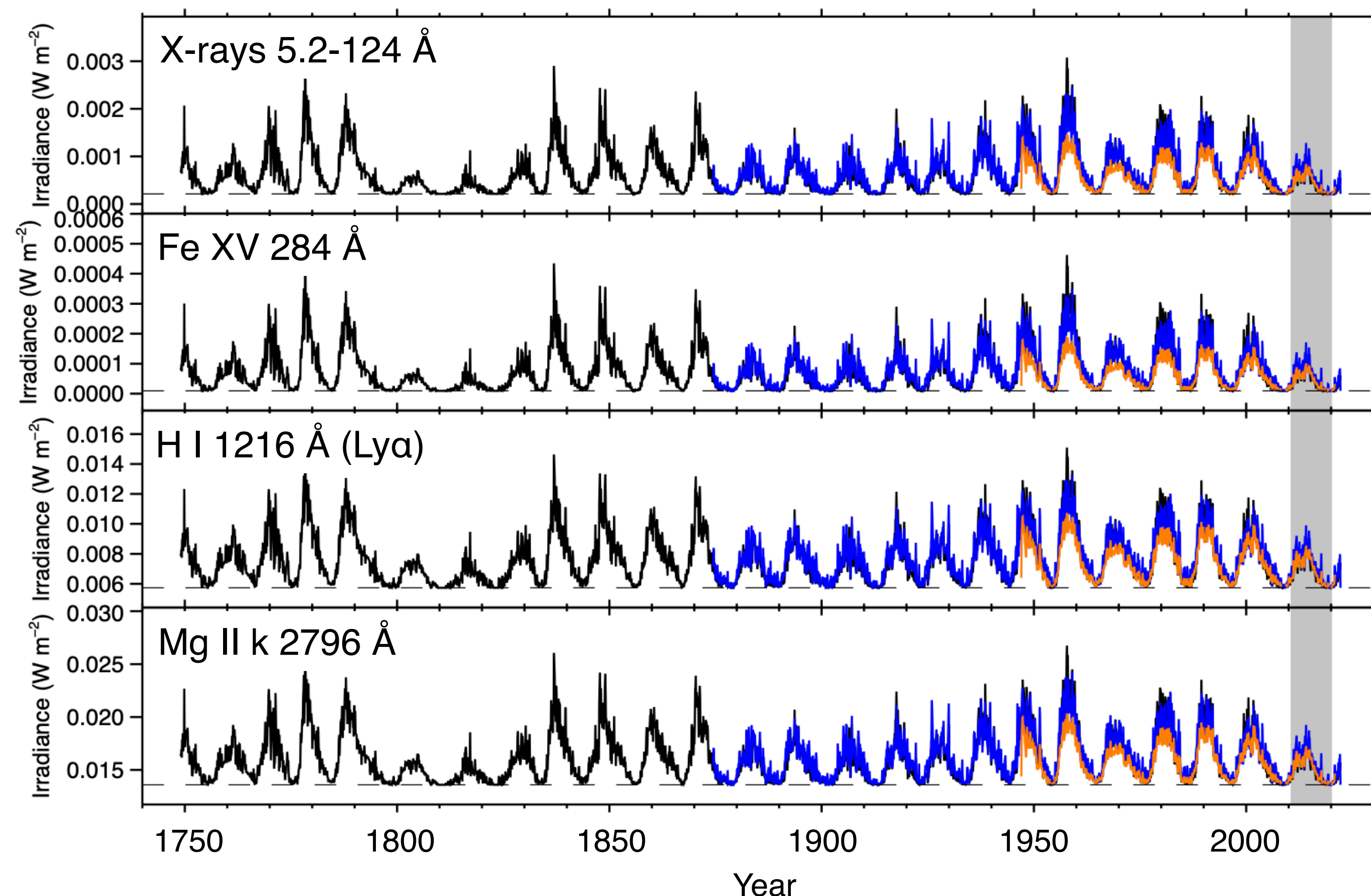
Irradiances can be reconstructed from

- Historical solar observations
- Stellar observations
- Surface flux transport simulations
- Dynamo models
- etc.

Pros: Relative differences between the proxies are less than 20% 🍷

Cons: Scalings are measured only for the “very weak” cycle 24 🍷

Sample reconstructed irradiances over centuries

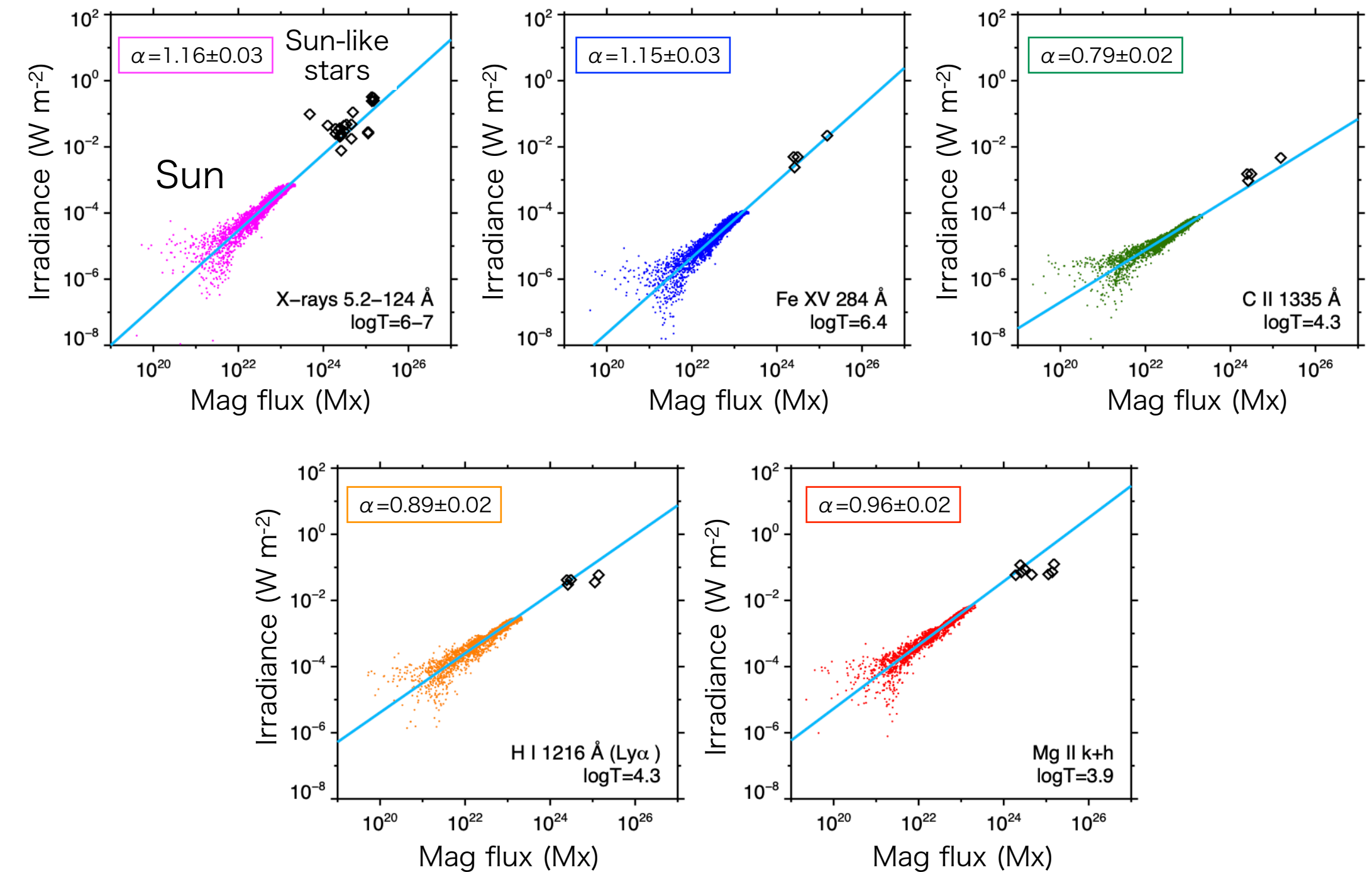


✓ New catalog provides means to empirically synthesize line irradiances

4. Summary and Discussion

- Characterization of stellar ARs
 - Test idea using Sun-as-a-star data
 - Long-term, multi-wavelength monitoring of stars may provide means to track AR evolutions
- Universal atmospheric heating
 - Comparison of scaling laws $F \propto \Phi^\alpha$ between the Sun and Sun-like stars with ages from 50 Myr to 4.5 Gyr
 - The heating mechanism is universal among the Sun and Sun-like stars, regardless of age or activity
 - Updated catalog of power-law index can be used for reconstruction of line irradiances from various proxy data

Mag flux—multi-line proportionality $F \propto \Phi^\alpha$



Toriumi et al. 2020, ApJ, 902, 36
Toriumi & Airapetian 2022, ApJ, 927, 179
Toriumi et al. 2022, ApJS, accepted

Thank you for your attention

Send feedback to toriumi.shin@jaxa.jp